

## Article

# Study on the Spatiotemporal Evolution and Influencing Factors of Forest Coverage Rate (FCR): A Case Study on Yunnan Province Based on Remote Sensing Image Interpretation

Renyi Yang<sup>1,2,3</sup> , Yimei He<sup>4</sup>, Changbiao Zhong<sup>1</sup>, Zisheng Yang<sup>2,3,\*</sup>, Xian Wang<sup>2,3</sup>, Mingjun Xu<sup>5</sup> and Linlin Cao<sup>2,3</sup>

<sup>1</sup> School of Economics, Yunnan University of Finance and Economics, Kunming 650221, China; 202203110030@stu.ynufe.edu.cn (R.Y.); zz1713@ynufe.edu.cn (C.Z.)

<sup>2</sup> Institute of Land & Resources and Sustainable Development, Yunnan University of Finance and Economics, Kunming 650221, China; 202102111545@stu.ynufe.edu.cn (X.W.); 202202111586@stu.ynufe.edu.cn (L.C.)

<sup>3</sup> Institute of Targeted Poverty Alleviation and Development, Yunnan University of Finance and Economics, Kunming 650221, China

<sup>4</sup> School of Tourism and Hospitality Management, Yunnan University of Finance and Economics, Kunming 650221, China; zz0974@ynufe.edu.cn

<sup>5</sup> College of Public Administration, Nanjing Agricultural University, Nanjing 210095, China; 2016209020@njau.edu.cn

\* Correspondence: zz0976@ynufe.edu.cn; Tel.: +86-138-8896-4270

**Abstract:** The study of the forest coverage rate (FCR) is related to the ecological environment and sustainable development goals (SDGs) of a region. In light of the lack of an organic integration method of “spatiotemporal evolution, correlation analysis, and change prediction” and the lack of a methodology that integrates methods of “remote sensing (RS) and GIS, multi-phase LUC, and construction of econometric models” in the research methods at present, this study focus on Yunnan, a typical border province located in China with a relatively fragile “innate” ecological environment, as the research area. Based on the interpretation of land use/land cover (LULC) data retrieved from seven periods RS images (1990, 1995, 2000, 2005, 2010, 2015, and 2020), the spatiotemporal evolution of FCR in 129 counties was analyzed. Complementary research methods, such as the spatial econometric model, geographically weighted regression (GWR), and the geographic detector (GD), are used to reveal the influencing factors of FCR. Finally, this study predicts the FCRs of 129 counties in Yunnan from 2025 to 2050. The FCR in Yunnan presents an increasing trend year by year, increasing from 28.96% in 1990 to 49.05% in 2020. In addition, it exhibits spatial agglomeration characteristics with fewer values in the east and more in the west. The analysis of influencing factors show that the increases in the per capita GDP, land utilization rate, and annual average temperature, and the implementation of the Conversion of Cultivated Land into Forest Project (CCFP) will significantly improve the FCR, while the increases in the population density land reclamation rate, the proportion of construction land area, and the proportion of soil erosion land area will significantly reduce the FCR. Furthermore, the FCR is influenced by multiple factors, and the relative factors observed not only show significant spatial differences, but also present complex and diverse patterns, with the additional characteristics of being interwoven and overlapping. This study contributes to expanding and improving the methods and pathways of exploring the spatiotemporal evolution characteristics of FCR in ecologically fragile areas using RS methods, providing a reference for increasing FCR and improving the ecological environment’s quality in Yunnan Province and other ecologically fragile areas.

**Keywords:** forest coverage rate (FCR); remote sensing (RS) image interpretation; influencing factors; ecological diversity; Yunnan Province



**Citation:** Yang, R.; He, Y.; Zhong, C.; Yang, Z.; Wang, X.; Xu, M.; Cao, L. Study on the Spatiotemporal Evolution and Influencing Factors of Forest Coverage Rate (FCR): A Case Study on Yunnan Province Based on Remote Sensing Image Interpretation. *Forests* **2024**, *15*, 238. <https://doi.org/10.3390/f15020238>

Academic Editors: Gilson Alexandre Ostwald Pedro da Costa, Raul Queiroz Feitosa, Veraldo Liesenberg and Claudio Almeida

Received: 3 January 2024

Revised: 21 January 2024

Accepted: 24 January 2024

Published: 26 January 2024



**Copyright:** © 2024 by the authors. Licensee MDPI, Basel, Switzerland. This article is an open access article distributed under the terms and conditions of the Creative Commons Attribution (CC BY) license (<https://creativecommons.org/licenses/by/4.0/>).

## 1. Introduction

Forests are not only important resources for human survival and development, but also have significant impacts on the economic, social, and ecological aspects (Chen Danlu et al., 2016; Zheng Yu et al., 2020; Bonan, G.B., 2008) [1–3]. Firstly, the contribution of forests to ecological protection is extremely significant. With the increase of forest coverage rate (FCR), it can not only effectively purify the air, but also prevent wind and sand, and maintain soil and water. According to the statistics, one hectare of forest resources can consume 1000 kg of CO<sub>2</sub> and release 730 kg of O<sub>2</sub> (Xiao Yanfei, 2020) [4]. According to a study conducted by Yang Renyi et al. (2022), under other unchanged conditions, every 1% increase of the FCR promotes a 0.0077% decrease of the air quality index (AQI) values [5]. In addition, the contribution of forests to economic and social development cannot be ignored, because forests not only are useful for wood production and processing, but also provide people with valuable medicinal materials and other material resources, which have an extremely important economic value and social benefits (Ran Xiaoou, 2016) [6]. It can be observed that forests are the cradle of human civilization and an indispensable material foundation for human survival and achieving sustainable development goals (SDGs). The FCR is a prominent indicator that reflects the richness of forests. Its calculation formula is the proportion of the forest area to the total land area, usually expressed as the ratio of a closed forest land area to the total land area (Yang Zisheng, 2011) [7], and some specially designated shrub forests can also be included in this calculation (Guan Yuxian, 2015) [8]. However, at present, China's FCR is only 23%, considerably less than the international average of 31.7%. Therefore, effectively improving the FCR is an urgent practice when attempting to achieve SDGs (Zhang Jitong et al., 2022) [9].

The research at present on forest coverage mainly includes the methods of dynamic monitoring (Hansen, M.C. et al., 2008) [10], spatiotemporal evolution analysis (Kennedy, R.E. et al., 2012; Cohen, W.B. et al., 2010) [11,12], influencing factor analysis (Wang Kai, 2016; Ma Jingjing et al., 2023) [13,14], and prediction (Verbesselt, J. et al., 2009; Pflugmacher, D. et al., 2012) [15,16], where dynamic monitoring mainly focuses on the detection of the changing dynamics of the FCR in a region through high-resolution RS satellite data; spatiotemporal evolution analysis is a method of systematically summarizing the features of spatial pattern and temporal changes based on FCR data from different years in different regions; the analysis of influencing factors mainly focuses on exploring the effects and degrees of various possible related factors on the FCR; and prediction focuses on the use of relevant modeling techniques based on existing data to predict the future FCR. Although these studies differ and focus on different aspects overall, in reality, they are all complementary and interrelated. For example, exploring the spatiotemporal evolution laws and influencing factors will help predict the future FCR, and the predicted results can further assist in dynamically monitoring whether the FCR deviates from expectations. In the past, due to the limitations in the fields of science and technology, the monitoring methods used to calculate FCR were relatively original. Their limitations mainly lie in the lack of precise equipment for monitoring the FCR, which may generate relatively coarse calculation results. With the growth and maturity of "3S" technology (i.e., remote sensing (RS) technology, geographic information systems (GISs), and global positioning systems (GPSs)), significant progress has been made in using "3S" technology to study FCR, and this has gradually become a hot topic in the research; it is evident that increasingly more abundant research results are emerging in the literature (Li Yang et al., 2018; Zhang Yangjian et al., 2022; Yin Huiyan et al., 2020) [17–19]. Overall, the existing research conducted on forest coverage mainly includes the following categories: The first category involves studying the spatiotemporal changes in FCR from the perspectives of land use/land cover change (LUCC) (Kennedy, R.E. et al., 2010; Gao Ying et al., 2019; Shi Ruyun et al., 2019; Zhang Weibo et al., 2022) [20–23]. The advantage of this type of research is the use of modern technologies, such as RS image interpretation, to accurately monitor the dynamic changes in FCR or relative indicators, and explore their evolution feature. However, its shortcoming is the inability to explore the relative factors of FCR. The second category is

the study of relative factors that affect forest coverage and its indicators (Li Qinling, 2023; Zhao Xiaodi et al., 2019; Wu Weiguang et al., 2023) [24–26]. The advantage of this type of research is that it can clearly reveal key indicators that affect FCR. From the existing research, it can be observed that the relative factors of FCR are quite complex, including not only economic factors (such as the GDP), but also the multiple impacts of social, policy (such as the Conversion of Cultivated Land into Forest Project (CCFP) and forest park constructions), population (such as population density and the natural population growth rate), and geographical condition (such as terrain slope and climate) (Wang Kai, 2016; Ma Jingjing et al., 2023; Kirton, J. et al., 2021; Brown, S. et al., 1984; Zhang Xiaodong, 2016; Deng Huiping et al., 2018; Wang Kai et al., 2016; Zhang Qian, 2016; Jiang Youyan et al., 2022) factors [13,14,27–33]. In addition, natural disasters and human activities can also become important influencing factors for the reduction in FCR, and the impacts of the relative factors are widely recognized in the literature (Hu Wenping et al., 2023; Mizuno, T. et al., 2021; Hefeeda, M. et al., 2009) [34–36]. However, the existing research conducted on the influencing factors lacks systematicity, with less use of diversified and complementary methods, such as econometric model analysis based on RS interpretation, resulting in most studies only focusing on one or a few aspects and failing to create a comprehensive study system of the influencing factors. The third category is the prediction of future FCR (Yang Zisheng, 2011; Pflugmacher, D. et al., 2012; Yuan Xue, 2022; Gu Kaiping, 1988) [7,16,37,38]. This type of research usually uses methods such as the back propagation (BP) neural network and Markov chain to predict future FCR, which can highlight the approximate changes in future FCR but fails to formulate more scientific predictions based on its core relative factors.

Overall, significant progress has been made in the existing research on the FCR, with more and more scholars conducting in-depth research on the dynamic monitoring, spatiotemporal evolution, influencing factors, and prediction of FCR. In addition, with the promotion of RS and GIS technologies, research methods have gradually diversified, such as integrating MODIS and Landsat data for dynamic monitoring, using diversified technologies such as the BP neural network, Markov chain, and Landsat-derived disturbance to predict FCR, and these research directions have gradually been integrated and expanded (Hansen, M.C. et al., 2008; Kennedy, R.E. et al., 2012; Cohen, W.B. et al., 2010; Wang Kai, 2016; Ma Jingjing et al., 2023; Verbesselt, J. et al., 2009; Pflugmacher, D. et al., 2012; Yuan Xue, 2022; Gu Kaiping, 1988) [10–16,37,38]. However, when exploring a literature review, it can be observed that there are still some shortcomings and the areas that required improvements and enhancements regarding the study of the influencing factors of FCR. In terms of the spatiotemporal evolution of FCR, many existing studies often use official statistical data, such as statistical yearbooks, for analyses, lacking the application of precise technical methods, such as RS image interpretation, to statistically analyze the land use types of each plot and achieve more accurate FCR monitoring results. In terms of the research conducted on the influencing factors, several existing studies mainly use methods such as principal component analysis and summarization, and lack the availability of a more comprehensive and systematic indicator system. As for the prediction research on FCR, many existing studies only use the trend of past changes in FCR to predict the future values, without dynamically adjusting future FCR based on the changes in the relative factors. Fortunately, with the growth and maturity of RS technology, more and more studies have used RS interpretation methods to systematically monitor FCR. This not only fills in the gaps mentioned above, but also continuously improves and innovates the technology, resulting in increasingly refined calculation results. However, this type of research mainly focuses on the accuracy of calculations and the improvement of methods, with less attention paid to the relevant factors and dynamic predictions of the FCR. Therefore, there is little organic integration of “spatiotemporal evolution, influencing factors, and change prediction” to form systematic and comprehensive analyses of FCR. At the same time, there is also a lack of understanding in the research regarding the spatial heterogeneity and interaction effects

of various relative factors on FCR, and a lack of a methodology that integrates the research methods of “RS and GIS, multi-phase LUCC, and construction of econometric models”.

Yunnan Province is located on the southwestern border of China and is a typical mountainous province with an underdeveloped economy and fragile ecological environment. This study adopts it as the research region, not only because it is a typical border mountain province, but also because it is located at the source or upstream of the six world-famous rivers (i.e., the Yangtze, Pearl, Lancang, Red, Nu, and Irrawaddy rivers), which means that Yunnan is not only an ecological security barrier located in southwest China, but it also has an irreplaceable and important role in maintaining the ecological security of the six world-renowned rivers. It can be observed that Yunnan’s important ecological location determines its significance as an international ecological security barrier. In response to the insufficient combining of the RS and GIS technology and econometric model analysis methods in the existing research to systematically explore the spatiotemporal evolution feature of FCR, and the lack of diversified and complementary measurement, techniques and methods combined with RS image interpretation results and econometric model analysis to systematically discuss the relative factors of FCR, this study analyzes the spatiotemporal evolution of FCR in 129 counties in Yunnan based on the LULC data obtained by the RS images for seven periods (i.e., 1990, 1995, 2000, 2005, 2010, 2015, and 2020). Complementary research methods, such as the spatial econometric models, the geographic weighted regression (GWR), and the geographic detector (GD), are combined to reveal the influencing factors on FCR. Finally, this study predicts the FCRs of 129 counties in Yunnan from 2025 to 2050. Compared with the existing research results, this study makes certain contributions: Firstly, it enriches and expands the systematic analysis of the “spatiotemporal evolution, influencing factors, and change prediction” of FCR in ecologically fragile areas by integrating the methods of “RS and GIS, multi-phase LUCC, and construction of econometric models”. The second contribution is the enrichment and expansion of the research methods and paradigms of interdisciplinary fields, such as econometrics and geography, to explore the important influencing factors, and the channels and methods for predicting future changes in FCR. Thirdly, this study provides a reference for the scientific formulation of policies and measures to successfully increase FCR and improve the ecological environment quality in Yunnan and other ecologically vulnerable areas according to the local conditions.

## 2. Materials and Methods

### 2.1. Overview of the Research Area

Yunnan is a border mountainous province located in southwestern China, with its latitude and longitude ranging from 21°8′32″ N to 29°15′8″ N and 97°31′39″ E to 106°11′47″ E, respectively (Figure 1). Overall, the features of Yunnan can be categorized into the following four points [39]:

The first is its frontier geographical location. Yunnan is located on the southwestern border of China, bordering Myanmar to the west and Laos and Vietnam to the south. The length of the border line is 3235.2 km. This geographical feature determines that Yunnan is located at the source or upstream of six major rivers, becoming an ecological security barrier.

Secondly, the terrain is mainly mountainous, making it a typical mountainous province. The overall terrain is characterized by a high northwest and low southeast. The highest point is 6740 m, and the lowest point is 76.4 m, with a height difference of 6663.6 m. The mountainous area of the entire province accounts for approximately 94% of the land, while the flat land only accounts for approximately 6%. About 77% of the land has a >15° slope, and nearly 2/5 of the land consists of steep slopes with a >25° slope. This topographic feature determines its vulnerability status in “innate” ecology. In addition, the long-lasting irrational development and utilization of land resources in mountainous areas can easily create disharmony in the relationship between human beings and the land, resulting in significant soil erosion and ecological degradation.

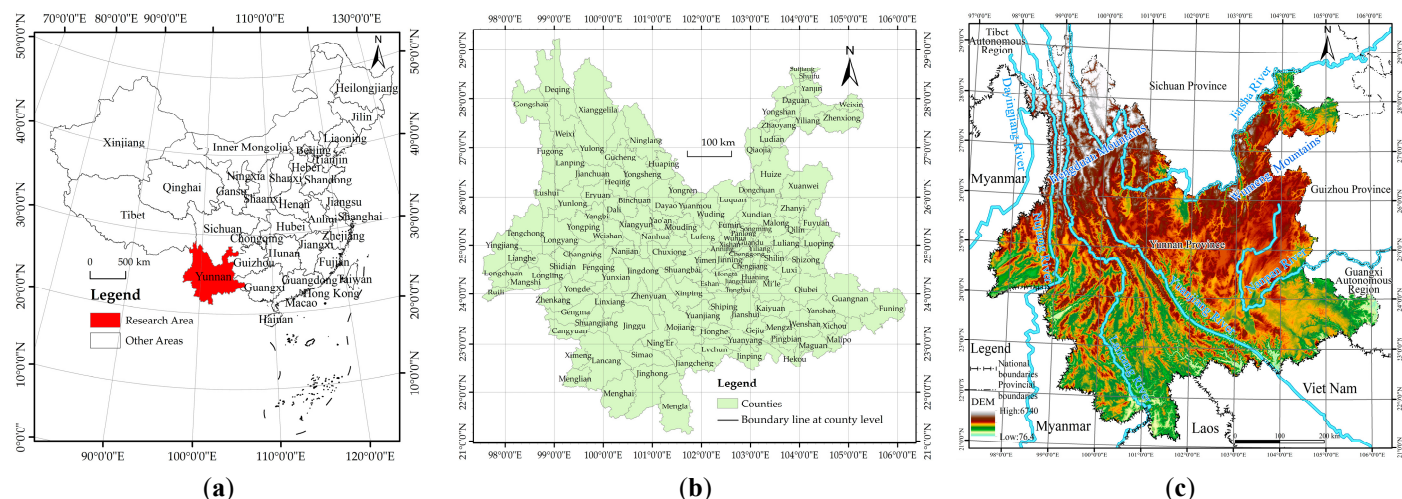


**Figure 1.** Geographical location and digital elevation model (DEM) map of the research area: (a) geographical location; (b) distribution of the 129 counties; and (c) DEM map.

Thirdly, there are numerous ethnic minorities living throughout Yunnan Province. There are a total of 55 ethnic minorities in China, and Yunnan Province has 51 ethnic minorities. Additionally, there are 25 ethnic minorities living in areas inhabited by ethnic minorities. In 2020, the population of ethnic minorities in Yunnan Province was 15.6396 million, accounting for approximately 1/3 of the total population in Yunnan. Various ethnic minorities have created diverse patterns of land use and ecological protection for their long-term survival and development.

Fourthly, the economy is underdeveloped. According to the statistics, the GDP of Yunnan in 2020 was CNY 245.22 billion, of which the output values of the primary, secondary, and tertiary industries accounted for 14.68%, 33.80%, and 51.53%, respectively [40]. In 2020, the per capita disposable income (PCDI) of all the residents living in Yunnan Province was CNY 23,295 (China's average is CNY 32,189), ranking in the 28th (fourth from the bottom) position in China, where the PCDIs of rural residents is CNY 12,842 (China's average is CNY 17,131) and also ranks 28th in China. In future development scenarios, while effectively protecting the ecology of the area, it is of great importance to vigorously develop the economy and steadily improve the PCDIs of all the residents.

## 2.2. Analysis Process and Steps

In general, the research steps in this article mainly include the following aspects (Figure 2):

(1) Using RS image interpretation to obtain the LULC data for Yunnan Province considering a total of 7 periods ranging from 1990 to 2020, and based on the interpretation results, this study obtained the FCRs in 129 counties.

(2) On the basis of extracting and calculating the FCR data, this study explores the laws and characteristics of their spatiotemporal evolution further, and refers to the existing research results to construct a scientific and reasonable indicator system of influencing factors based on the data obtained from the RS image interpretation, statistical yearbooks, relevant functional department surveys, and other channels.

(3) This study uses complementary econometric model analysis techniques, such as the spatial econometric models, the GWR, and the GD to analyze influencing factors of FCR. When analyzing the influencing factors, they included not only the effect of the influencing factors, but also the differences in their effects and the interaction effects of different overlapping influencing factors.

(4) By using econometric models, this paper will predict the FCRs of 129 counties in Yunnan from 2025 to 2050.

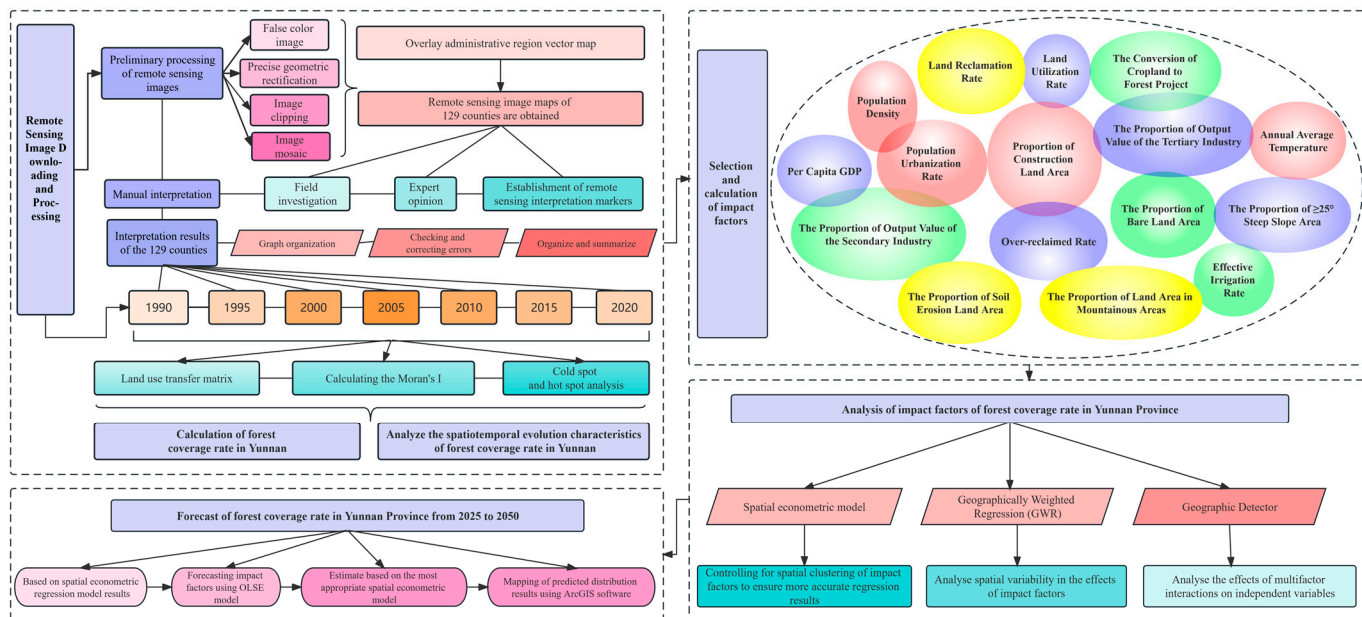


Figure 2. Research steps and processes.

### 2.3. RS Image Interpretation Data Acquisition and Explanation

The RS image data of the 7 periods (i.e., 1990, 1995, 2000, 2005, 2010, 2015, and 2020) used in this study are available at the following website: “<https://www.resdc.cn/>”, accessed on 18 January 2023.

The Chinese Academy of Sciences (CAS) established a multi-period LULC RS image database of China. In terms of seasonality, this study selected images with winter cloud cover of less than 10% for the interpretation (Table 1).

Table 1. Detailed information of the RS images from 1990 to 2020.

Year	RS Image Data Details	Time	Spatial Resolution
1990	Landsat TM	Dec 1989 to Feb 1992	30 m × 30 m
1995	Landsat TM	Dec 1995 to Feb 1996	
2000	Landsat TM/ETM	Dec 1999 to Feb 2000	
2005	Landsat TM/ETM	Dec 2004 to Feb 2005	
2010	Landsat TM	Dec 2009 to Feb 2010	
2015	Landsat-8	Jan 2015 to Feb 2015	
2020	Landsat-8	Jan 2020 to Feb 2020	

The seven-phase land use vector database of Yunnan was obtained through interactive human–machine interpretation and interpretation of LULC types based on the unified land use classification system and the RS interpretation markers within the ArcGIS 10.5 software environment. The specific steps were as follows:

- (1) After obtaining the RS images, this study first performed image preprocessing operations, such as the false color synthesis, precise geometric rectification, image clipping, and image mosaic, and then overlaid the administrative vector maps of 129 counties in 2021 to obtain the RS image maps for each county.
- (2) Based on the field investigations and comprehensive expert opinions, this study established RS image interpretation markers suitable for Yunnan Province, and also obtained DEM, vegetation, and land use maps, and then performed manual interpretations.
- (3) During the interpretation process, the counties were used as units to generate interpretation results for each county.
- (4) After the interpretation was completed, this study used the “Arcinfo Workstation” and “SHAPEARC” commands to generate the “coverage” files for each county. Finally, this

study used the ARCEDIT module of ARC/INFO to edit the graphics, check and modify errors, and then organized and summarized the results.

(5) Finally, referring to the research conducted by Xu Xinliang et al. (2018) [41], Liu Jiyuan et al. (2002, 2003, 2014) [42–44], and Kuang Wenhui et al. (2022) [45], this study divided them into 6 primary and 12 secondary land types, and calculating the land areas of 6 primary and 12 secondary land types for each county for the 7 periods (Table 2).

**Table 2.** Classified areas of LULC areas in Yunnan Province in 1990, 1995, 2000, 2005, 2010, 2015, and 2020.

Land Use Types		Land Use Classification Area (Unit: 10,000 Hectares)						
Number	Name	1990	1995	2000	2005	2010	2015	2020
1	Cultivated Land	552.45	551.27	551.08	548.89	545.96	542.28	539.56
11	Paddy Field	136.77	136.24	135.91	135.37	134.53	132.68	131.39
12	Dryland	415.68	415.03	415.17	413.52	411.43	409.60	408.17
2	Woodland	1868.92	1930.96	1998.19	2119.85	2224.10	2321.67	2418.67
21	Closed Forest Land	1112.91	1237.20	1414.58	1553.96	1724.81	1784.48	1884.72
22	Other Forest Land	756.02	693.75	583.61	565.89	499.29	537.19	533.95
3	Grassland	532.64	501.25	481.25	403.85	325.65	253.64	181.12
31	Pasture with High Coverage	340.02	323.92	307.02	248.01	195.20	150.60	105.36
32	Pasture with Medium and Low Coverage	192.62	177.33	174.23	155.84	130.46	103.04	75.76
4	Waters	48.14	48.52	49.34	51.14	53.28	54.75	56.09
41	Rivers and Lakes	31.96	31.86	31.78	31.63	31.47	31.32	31.18
42	Reservoirs and Ponds	16.18	16.66	17.56	19.51	21.81	23.43	24.91
5	Construction Land	61.78	64.10	66.72	76.77	86.77	108.00	129.69
51	Urban Construction Land, Rural Settlement Area, and Land for Mining and Industry	50.82	52.72	54.84	61.94	71.86	90.40	109.17
52	Other Building Land	10.96	11.38	11.88	14.82	14.91	17.59	20.52
6	Unused Land	778.48	746.33	695.85	641.93	606.67	562.09	517.30
61	Bare Land	105.56	100.61	96.13	83.44	70.73	67.64	64.83
62	Other Land Types	672.92	645.72	599.72	558.49	535.93	494.46	452.47

The LULC classification results obtained from the interpretation of the 7 phases' RS image data are in line with reality. Taking the 2020 LULC classification results as an example, compared with the *Main Data Bulletin of the Third National Land Survey of Yunnan Province*, which was compiled by the Office of the Leading Group of the Third National Land Survey of Yunnan Province on 31 December 2019, the total cultivated land area of the province interpreted by RS in 2020 was 5.3956 million hectares, while the total cultivated land area of Yunnan Province in 2019 from the Third National Land Survey of Yunnan Province (TNLS) was 5.3955 million hectares, which is relatively close. The total forest area of the province interpreted by RS in 2020 was 24.1867 million hectares, while the total forest area of TNLS in 2019 was 24.97 million hectares, with a difference of only 3.16% between the two. The total construction land area of the province interpreted by RS in 2020 was 1.2969 million hectares, while TNLS's total construction land area in 2019 was 1.302 million hectares, with a difference of only 0.25%. It can be seen that the LULC classification in this RS interpretation is relatively accurate.

Based on the results obtained from the RS image interpretation (Table 2), this study calculated the FCRs (dependent variables) of 129 counties in Yunnan Province from 1990 to 2020 and analyzed their spatiotemporal evolution features. At the same time, other independent variables related to ecology and land use (such as the land reclamation rate, land utilization rate, the proportion of construction land and the proportion of bare land

areas, and effective irrigation rate) were also established. Based on the other available data of *Yunnan Statistical Yearbook*, existing thematic surveys, the second national land survey in Yunnan Province dam area special survey, and special survey of land area in different climatic zones and slopes in Yunnan Province and various meteorological stations in China, a scientific, reasonable, and rich indicator system of the influencing factors of FCR was constructed. Combined with other spatial econometric models, a comprehensive and scientific analysis of the influencing factors was conducted by using diversified and complementary methods.

#### 2.4. Construction and Model Analysis of the Influencing Factor Indicator System

##### 2.4.1. Construction of the Influencing Factor Indicator System

The data collected in this study are panel data. Prior to the construction of the model, it was necessary to clarify the dependent variable and determine the relevant independent variables based on the existing relevant theories and empirical research to form a scientific and reasonable indicator system for the analysis of the influencing factors.

The dependent variable of this study was the FCRs of 129 counties ranging from 1990 to 2020, and the data were sourced from RS image interpretations. When analyzing the influencing factors of FCR, considering that the existing studies concerning influencing factors only rely on relatively single sources of data, such as statistical yearbooks, and lack the use of RS interpretations of LULC and survey statistical data from relevant institutions, this study constructs relevant indicator systems and determines the relevant influencing factors of FCR by referring to the research conducted by Kirton, J. et al., 2021; Brown, S. et al., 1984; Zhang Xiaodong, 2016; Deng Huiping et al., 2018; Wang Kai et al., 2016; Zhang Qian, 2016; and Jiang Youyan et al. 2022 [27–33]. Based on a summary of the shortcomings and research trends of the existing research on influencing factors of FCR, this study incorporated the existing research approaches and selection of reasonable indicators for successfully measuring land use and ecological protection when using the RS image interpretation method (Yang Zisheng et al., 2023) [46]. In addition, this study referred to the indicator systems of industrial economy and population structure presented by Yang Renyi et al. (2022) [5] and He Bowen et al. (2019) [47] when studying urbanization and economic development, as well as the indicator system and research methods used by Yang Zisheng et al. (2021) [48] in exploring the influencing factors of resource environment and geographical conditions. Moreover, this study constructed an indicator system from five dimensions (Table 3). Considering that most economic and social indicators exhibited exponential growth characteristics and that it was not conducive to construct linear regression models to explore the actual impacts of these economic indicators during analyses, this study referred to the methods of Yang Renyi et al. (2022) [5], and introduced the natural logarithmic forms of the PCGDP and PD (Table 3).

As shown in Table 3, the data for the industrial economy and population structure were sourced from the Yunnan Statistical Yearbook and Express Professional Superior (EPS) platform (website: "<https://www.epsnet.com.cn/index.html#/Index>", accessed on 9 October 2023). Due to regional adjustments, the county-level data for Gucheng and Yulong from 1990 to 2000 were converted and supplemented based on the proportion in 2005. The FCRs and main data for other dimensions were obtained from RS image interpretations. Considering that, since CCFP in Yunnan Province were introduced in 2000, the conversion of a certain area of steep slope cultivated land into forest land in various counties of Yunnan Province would increase the FCR. This study introduced a dummy variable named  $P_{CCF}$ , to explore the policy effects of CCFP. In addition, this study referred to the method employed by Yang Renyi et al. (2022) [5] and used the IDW method to spatially interpolate the data obtained from various meteorological stations in China to determine the annual average temperature and precipitation data. Considering that the data included some indicators that did not change over time (such as  $P_{MA}$  and  $P_{SSA}$ ), which were key geographical factors affecting the FCR, this article adopted the random effects (RE) model to analyze the relevant influencing factors.



**Table 3.** Index system of the influencing factors of the FCR.

Attributions	Dimensions	Variables	Names	Calculation Methods	Data Sources	Units
Influence Factors	Dependent Variable	Forest Coverage Rate (FCR)	$F_{CR}$	Closed Forest Land Area/Total Land Area $\times$ 100%	RS Image Interpretation	%
	Industrial Economy	Per Capita GDP (PCGDP)	$\ln P_{GDP}$	$\ln(\text{Gross Domestic Product (GDP)/Total Population})$	Yunnan Statistical Yearbook	CNY/Person
		The Proportion of Output Value of the Secondary Industry	$P_{OSI}$	Output Value of the Secondary Industry/GDP $\times$ 100%	Yunnan Statistical Yearbook	%
		The Proportion of Output Value of the Tertiary Industry	$P_{OTI}$	Output Value of the Tertiary Industry/GDP $\times$ 100%	Yunnan Statistical Yearbook	%
	Population Structure	Population Density (PD)	$\ln P_D$	$\ln(\text{Total Population/Total Land Area})$	Yunnan Statistical Yearbook	Person/km <sup>2</sup>
		Population Urbanization Rate	$P_{UR}$	(1-Total Rural Population)/Total Population $\times$ 100%	Yunnan Statistical Yearbook	%
	Land Use	Land Reclamation Rate	$R_{LR}$	Cultivated Land Area/Total Land Area $\times$ 100%	RS Image Interpretation	%
		Proportion of Construction Land Area	$P_{CLA}$	Construction Land Area/Total Land Area $\times$ 100%	RS Image Interpretation	%
		Land Utilization Rate	$R_{LU}$	(1-Unused Land Area/Total Land Area) $\times$ 100%	RS Image Interpretation	%
		The Conversion of Cultivated Land to Forest Project (CCFP)	$P_{CCF}$	Taking 1 in 2000 and Later, and Taking 0 in Other Years	None	None
	Ecological Protection	Over-reclaimed Rate	$R_{OR}$	(Land Reclamation Rate—Suitable Land Reclamation Rate)/Suitable Land Reclamation Rate $\times$ 100%	RS Image Interpretation, Land Suitability Evaluation	%
		The Proportion of Bare Land Area	$P_{BLA}$	Bare Land Area/Total Land Area $\times$ 100%	RS Image Interpretation	%
		The Proportion of Soil Erosion Land Area	$P_{SE}$	Soil Erosion Area/Total Land Area $\times$ 100%	Existing Thematic Surveys	%
	Natural Environmental Conditions	Effective Irrigation Rate	$R_{EI}$	Paddy Field Area/Cultivated Land Area $\times$ 100%	RS Image Interpretation	%
		The Proportion of Land Area in Mountainous Areas	$P_{MA}$	Land Area in Mountainous Areas/Total Land Area $\times$ 100%	The Second National Land Survey in Yunnan Province Dam Area Special Survey	%
		The Proportion of $\geq 25^\circ$ Steep Slope Area	$P_{SSA}$	$\geq 25^\circ$ Steep Slope Area/Total Land Area $\times$ 100%	Special Survey of Land Area in Different Climatic Zones and Slopes in Yunnan Province	%
		Annual Average Temperature	$A_{AT}$	Convert to Grid Data with a Resolution of $0.1^\circ \times 0.1^\circ$	Data from Various Meteorological Stations in China	$^\circ\text{C}$
	Annual Average Precipitation	$A_{AP}$	using the IDW Interpolation Method		mm	

### 2.4.2. Introduction of Spatial Econometric Models

The theory suggests that the ordinary least squares (OLS) estimation could fail when used for data with spatial correlations, and, thus, requires the use of spatial econometric methods for estimation (Chen Qiang, 2014) [49]. Its main steps include establishing a spatial weight matrix  $W$ , calculating Moran’s  $I$ , conducting a model estimation and analysis,

drawing conclusions, and then applying them. The formula for Moran's I is as follows (Moran P, 1950) [50]:

$$\text{Moran's } I = \frac{n\mathbf{e}^T\mathbf{W}\mathbf{e}}{\mathbf{e}^T\mathbf{e}\left(\sum_i\sum_j w_{ij}\right)} = \frac{\sum_i\sum_j w_{ij}(x_i - \bar{x})(y_i - \bar{y})}{S^2\left(\sum_i\sum_j w_{ij}\right)} \quad (1)$$

where  $\mathbf{e}$  is the residual matrix,  $\mathbf{W}$  is the spatial weight matrix, and  $S^2$  is the variance of the observed value  $x_i$ . The value of Moran's I generally ranges from  $-1$  to  $1$ . The closer the value is to  $-1$ , the more obvious the degree of dispersion is; the closer it is to  $1$ , the more obvious the degree of aggregation is; and the closer it is to  $0$ , the more obvious the degree of randomness is. After the transformation, it approximately follows a normal distribution; thus, it can conveniently be used to determine spatial correlation.

The principle of Geary's C is similar to Moran's I (Gear R, 1954) [51]; however, due to the inability of these two indices to distinguish between the "hot spot" and "cold spot", Getis and Ord (1992) [52] propose the indicator of Getis–Ord  $G_i^*$ :

$$\text{Getis - Ord } G_i^* = \frac{\sum_{i=1}^n \sum_{j=1}^n w_{ij} x_i x_j}{\sum_{i=1}^n \sum_{j \neq i}^n x_i x_j} \quad (2)$$

The common spatial econometric panel models include the SAC model (spatial autocorrelation), SEM (spatial error model), SAR model (spatial autoregressive), and SDM (spatial Durbin model). For static panels, the general nesting spatial model can generally be represented as follows (Yang Zisheng et al., 2021) [48]:

$$\begin{aligned} \mathbf{Y} &= \rho\mathbf{W}_1\mathbf{Y} + \mathbf{X}\boldsymbol{\beta} + \mathbf{W}_2\mathbf{X}\boldsymbol{\delta} + \mathbf{u} + \boldsymbol{\gamma} + \boldsymbol{\varepsilon}, \\ \boldsymbol{\varepsilon} &= \lambda\mathbf{W}_3\boldsymbol{\varepsilon} + \mathbf{v} \end{aligned} \quad (3)$$

where  $\rho$  and  $\lambda$  represent spatial parameters;  $\boldsymbol{\delta}$  represents fixed and unknown parameter vectors that need to be estimated (due to  $\mathbf{W}_2\mathbf{X}\boldsymbol{\delta}$  indicating the spatial lag of the dependent variable, the coefficient estimated value of  $\boldsymbol{\delta}$  is usually used to calculate spatial spillover effects);  $\mathbf{W}_1$ ,  $\mathbf{W}_2$ , and  $\mathbf{W}_3$  represent spatial weight matrices;  $\mathbf{Y}$  represents the vector matrix of the FCR;  $\mathbf{X}$  represents the independent variable matrix;  $\boldsymbol{\beta}$  represents the parameter vector (i.e., the estimated coefficients of each independent variable, which is used to study the specific impact of the relative variables on FCR);  $\mathbf{u}$  represents the individual effect;  $\boldsymbol{\gamma}$  represents the time effect;  $\boldsymbol{\varepsilon}$  represents a random error vector; and  $\mathbf{v}$  represents a normally distributed random error vector. Static panels typically use SARAR, SAR or the SEM models. If  $\boldsymbol{\delta} = \mathbf{0}$ , it is called the SAC model, which generally focuses on fixed effects estimations and is not suitable for random effects estimation and analysis. If  $\boldsymbol{\delta} = \mathbf{0}$  and  $\lambda = 0$ , it is called the SAR model. If  $\boldsymbol{\delta} = \mathbf{0}$  and  $\rho = 0$ , it is called the SEM model. The SDM is generally used to estimate spatial spillover effects and is less involved in determining influencing factors [48,53]. Therefore, the SAC, the SAR and the SEM models are usually used in the research, and it is necessary to select the most suitable model based on the statistical indicators or parameters, such as LM-lag, LM-error, robust LM-lag, robust LM-error, or the Moran's I error term.

#### 2.4.3. Introduction of the Geographically Weighted Regression (GWR) Model

The GWR model is a spatial regression model proposed by Fotheringham et al. (1999) based on the idea of local smoothness [54]. It incorporates the spatial attributes of the data into the regression model, allowing the values of the variables to be changed with the spatial positions, thereby reflecting the spatial non-stationary nature of parameters in different regions [55,56]. Specifically, it is set as follows [57]:

$$y_i = \beta_0(u_i, v_i) + \sum_{k=1}^p \beta_k(u_i, v_i)x_{ik} + \varepsilon_i, i = 1, 2, \dots, n \quad (4)$$

where  $y_i$  is the observed value of the FCR in the county  $i$  and  $x_{ik}$  is the observed value of the independent variable  $k$  in the county  $i$ ;  $\beta_0$  is the intercept coefficient;  $\beta_k$  is the coefficient of the independent variable  $k$  in the county  $i$ ; and  $\varepsilon_i$  is the random error term.

In practical operations, it requires the original data to be cross-sectional. In this paper, the average variable values of each year were used as the data ( $P_{CCF}$  was a 0–1 variable, so it was not included in the GWR model estimation).

#### 2.4.4. Introduction of the Geographic Detector (GD)

The GWR model is limited to measuring the degree of the individual impact of a single factor, while the geographic detector (GD) can measure the degree of the joint impact of two influencing factors on FCR [58,59]. The explanatory power of factors in the GD is measured by the  $Q$  value [60]:

$$Q = 1 - \frac{\sum_{h=1}^L N_h \sigma_h^2}{N \sigma^2} \tag{5}$$

where  $L$  represents the stratification of the FCR or influencing factors (i.e., classification or zoning);  $N_h$  and  $\sigma_h^2$  represent the number of units and variance of layer  $h$ , respectively; and  $N$  and  $\sigma^2$  represent the overall number of units and variance. The  $Q$  value represents the influencing degree on the FCR, ranging from 0 to 1. The relationship between two factors can be classified into 5 types (Wu Peng et al., 2018) [57] (Table 4).

**Table 4.** Judgment basis for different interactions of GD interactions.

Judgment Basis	Interaction Types
$Q_{x1 \cap x2} < \min(Q_{x1}, Q_{x2})$	Non-linear Attenuation (NA)
$\min(Q_{x1}, Q_{x2}) < Q_{x1 \cap x2} < \max(Q_{x1}, Q_{x2})$	Single-Factor Non-Linear Attenuation (SNA)
$Q_{x1} + Q_{x2} > Q_{x1 \cap x2} > \max(Q_{x1}, Q_{x2})$	Double-Factor Enhancement (DE)
$Q_{x1 \cap x2} = Q_{x1} + Q_{x2}$	Independent of Each Factor (IF)
$Q_{x1 \cap x2} > Q_{x1} + Q_{x2}$	Non-Linear Enhancement (NE)

In practical operations, the GD and GWR model have similar data requirements (i.e., requiring the panel data to be converted into cross-sectional data). Therefore, this study employed the average values of each year as the sample data ( $P_{CCF}$  was a dummy variable, so it was not included in the model estimation). Before using the GD to explore the interaction of influencing factors, it was necessary to normalize and classify each influencing factor. Considering that the influencing factors involved in this article were positively and negatively correlated with the FCR, this study referred to the research method employed by He Bowen et al. (2019) [47] when normalizing the influencing factors with positive (+) and negative (−) attributions, and respectively processed them as dimensionless to convert them into values with a range of [0, 1] (the  $F_{CR}$  was the dependent variable in this study, with a range of 0 to 100, which could be divided by 100 to obtain values with a range of [0, 1]):

$$q_{ij} = \frac{X_{ij} - \min(X_j)}{\max(X_j) - \min(X_j)} \text{ OR } q_{ij} = \frac{\max(X_j) - X_{ij}}{\max(X_j) - \min(X_j)} \tag{6}$$

where  $X_{ij}$  represents the original value of the index  $j$  in the county  $i$ , and  $q_{ij}$  is the dimensionless attribute value of the index  $j$  in the county  $i$ ; and  $\max$  and  $\min$  represent the maximum and minimum values of the index, respectively.

In addition, data classification was required before using the GD method. This study divided each indicator into 5 categories based on the natural breakpoint method (NBM). The NBM, also known as the Jenks Method, is a classification method aimed at arranging a set of numerical optimizations into “natural” classes. This method is based on the principle of univariate classification in cluster analysis. When the number of levels is determined, the data breakpoints between classes are iteratively calculated to minimize the differences within the same category and maximize the differences among different categories, thereby

grouping the similar values in the data most appropriately (Huang Qi et al., 2023) [61]. The NBM has been widely applied in research such as GWR and GD (He Bowen et al., 2019; Wu Peng et al., 2018) [47,57].

### 2.4.5. Predictive Analysis of Econometric Models

Econometric models not only estimate the results of specified parameters, but also make reasonable predictions for the future. Common prediction models include OLS, autoregression (AR), moving average process (MA), and vector autoregression (VAR) (Chen Qiang, 2014) [49]. Considering that the data type used in this study was panel data, the spatial econometric models could effectively control and eliminate the interference of data with spatial autocorrelation issues on the results, thereby obtaining more accurate estimation results. Applying this estimation method to the prediction analysis can result in more scientific and reliable prediction results for future FCRs. Referring to the research ideas and methods of Chen Qiang (2014) [49] and Yang Renyi et al. (2021) [62], this study used the OLS method to predict the results of various influencing factors from 2025 to 2050 ( $P_{CCF}$  takes 1 in 2000 and later), and based on the selection of the most suitable model to fit the panel data from 1990 to 2020, this study predicted the FCRs of 129 counties in Yunnan Province from 2025 to 2025.

## 3. Results

### 3.1. Analysis of the Spatiotemporal Evolution of the FCR

#### 3.1.1. Analysis of the Spatiotemporal Evolution of the FCR over the Past 30 Years

According to the results this study obtained, the closed forest land area in Yunnan shows a trend of increasing from 11.1291 million hectares in 1990 to 18.8472 million hectares in 2020, with a net increase of 69.35% over 30 years and an average annual growth rate of 1.77%. This means that the overall FCR increased from 28.96% (in 1990) to 49.05% (in 2020), with a net increase of 20.09%. It can be observed that the FCR in Yunnan is gradually increasing, and with the increase in people’s awareness of the ecological civilization construction (ECC) concept, the inherently fragile ecological environment is gradually improving, and new progress regarding the ECC will be achieved.

The aforementioned RS interpretation results intuitively show the trend of changes occurring in closed forest land area and FCR in Yunnan in the past 30 years. However, to analyze the reasons for the increase in FCR more thoroughly, it is necessary to understand the extent to which other land use types (LUTs) has transformed into closed forest land in the past 30 years, and how much of the original closed forest land has transformed into other LUTs. Therefore, this study calculated the transfer matrices of LUTs (Table 5).

**Table 5.** Transfer matrices of LUTs in Yunnan Province from 1990 to 2020 (unit: 10,000 hectares).

Number of Types	1990	The Area of Mutual Transformations of Various LUTs							Decrease	2020
		→1	→21	→22	→3	→4	→5	→6		
1	552.45	520.13	7.52	4.32	5.05	2.61	10.24	2.58	32.33	539.56
21	1112.91	6.38	1074.34	13.60	4.99	1.12	11.64	0.83	38.56	1884.72
22	756.02	4.28	245.48	480.31	7.56	2.02	16.32	0.04	275.71	533.95
3	532.64	5.33	374.55	1.13	127.46	1.22	22.65	0.30	405.18	181.12
4	48.14	0.44	0.08	0.03	0.35	46.77	0.39	0.06	1.37	56.09
5	61.78	0.31	0.22	0.07	0.10	1.31	59.65	0.13	2.13	129.69
6	778.50	2.69	182.53	34.49	35.61	1.04	8.80	513.35	265.15	517.30
Total	3842.42	539.56	1884.72	533.95	181.12	56.09	129.69	517.30	—	3842.42
—	Increase	19.44	810.38	53.64	53.66	9.32	70.04	3.95	—	—
—	Net Increase or Decrease	−12.89	771.81	−222.07	−351.52	7.95	67.91	−261.20	—	—

Note: In the number of land use types, 1, 2, 3, 4, 5, and 6 represent cultivated land, woodland, grassland, water, construction land, and unused land, respectively; where, 21 and 22 represent closed forest land (CFL) and other forest land, respectively.

It can be seen that, although there were nearly 0.3856 hectares of closed forest land (CFL) converted to other LUTs during the past 30 years, there are still 8.1038 million hectares of other LUTs converted to the CFL (Table 5). Due to the significantly higher value of the latter, the net increase in the CFL was 7.7181 million hectares from 1990 to 2020. Where there was a considerable amount of CFL area that was converted to other forest land and construction land, reaching  $1.36 \times 10^5$  (35.27%) and  $1.16 \times 10^5$  (30.19%) hectares, respectively. This means that a considerable amount of land was converted from closed forest land into sparse shrubs and other forest land, and even into construction land. This also indicates that there are still some unreasonable land use phenomena in the urbanization process. Fortunately, there are still many other LUTs that have been converted into CFL. The areas of cultivated land, other forest land, grasslands, water bodies, construction land, and unused land converted into CFL were  $7.52 \times 10^4$  (0.93%),  $2.45 \times 10^6$  (30.29%),  $3.75 \times 10^6$  (46.22%), 800 (0.01%),  $2.2 \times 10^3$  (0.03%), and  $1.83 \times 10^6$  (22.52%) hectares, respectively. This means that the areas of land converted from other forest land, grasslands, and unused land to CFL were very large, accounting for 99.03% of the total increase of the reason why  $8.03 \times 10^6$  hectares of other forest land, grassland, and unused land have been converted into CFL is due to the effectiveness of afforestation. Yunnan has continuously increased the proportion of its closed forest area, significantly increased its FCR and improved its ecological environment in the past 30 years, achieving great results in terms of the ECC.

Although the aforementioned method calculates the overall FCR, CFL area, and LUCC in Yunnan, the spatiotemporal evolution of the FCR remain unexplored. To display the changes in the FCRs of 129 counties more intuitively, this study draws the FCR distribution maps of seven periods in 129 counties based on the RS interpretation results (Figure 3).

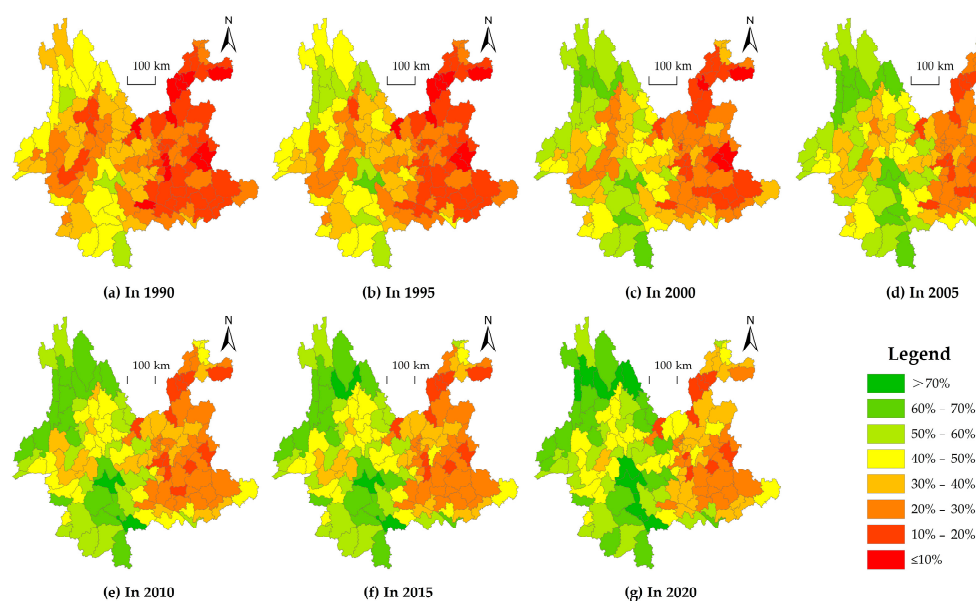


**Figure 3.** RS interpretation results for FCRs of 129 counties in Yunnan Province from 1990 to 2020.

From Figure 3, two basic conclusions can be drawn:

(1) From the perspective of analyzing spatial patterns, the FCR in Yunnan generally presents a trend of lower in the east and higher in the west, which occurs regardless of how the FCR changes from 1990 to 2020. The reason for this result is related to the geographical conditions of Yunnan Province: there are many areas located in the southeast under the jurisdiction of some prefectures (such as Honghe and Wenshan) suffering from karst rocky desertification, mostly exposed rocks, and unused land. However, as a result of afforestation, the FCRs in these areas have gradually improved. The central region of Yunnan represents an important growth pole, presenting more developed economic

conditions compared to other regions, such as Chuxiong, Kunming, and Qujing, which have a better overall economic outlook and more construction land, thus greatly affecting the FCR. The overall altitude, steep slopes, and low population density in Diqing, Nujiang, Lijiang, and other counties in the northwest region result in relatively high FCRs. Moreover, with the promotion of the CCFP in 2000, steep slope farmland in these areas has been transformed into forest land, which has significantly promoted the increase in the FCR. The temperatures in Dehong in the west and Xishuangbanna in the southwest are relatively high and there is sufficient precipitation, and the ecological environment is also relatively good, so the FCR is relatively high.

(2) From the perspective of time changes, the FCRs in various counties in Yunnan have generally improved in the past 30 years, and their ecological environments have also greatly improved. In 1990, Luoping presented the lowest value among the 129 counties, with the  $F_{CR}$  value of only 5.37%; the county with the highest value was Zhenyuan, with the  $F_{CR}$  value of only 55.52%. In 1990, there were 12 counties with  $F_{CR}$  values less than or equal to 10%, accounting for 9.30%; there were 36 counties with  $F_{CR}$  values of 10% to 20%, accounting for 27.91%; and only 3 counties, accounting for 2.33%, had  $F_{CR}$  values of over 50%. In 2020, Chenggong presented the lowest value out of the 129 counties, with the  $F_{CR}$  value of 12.53%; the county with the highest value was Yulong, with the  $F_{CR}$  value of 76.02%. In 2020, there were no counties with the  $F_{CR}$  value less than or equal to 10%; only 9 counties with  $F_{CR}$  values of 10% to 20%, accounting for 6.98%; and 52 counties, accounting for 40.31%, with  $F_{CR}$  values over 50%. From the comparison of the results between 1990 and 2020, not only did the values of the counties with the lowest/highest  $F_{CR}$ s significantly increased, but the number of counties with the low  $F_{CR}$ s significantly decreased, and the number of counties with the high  $F_{CR}$ s significantly increased. Ultimately, the FCRs of various counties in Yunnan significantly improved.

From the results presented above, it can be seen that the FCRs of the 129 counties present a clear spatial distribution pattern, showing an overall trend of appearing lower in the east and higher in the west. In order to explore the relevant influencing factors, it is necessary to use spatial econometric models to better control the interference caused by spatial agglomeration. However, Figure 3 presents the spatial distribution characteristics intuitively, and whether it has the significant clustering characteristics still require more precise calculations and analyses by using reasonable statistical methods.

### 3.1.2. The Spatial Distribution Patterns of the FCRs in 129 Counties in Yunnan Province

To more precisely measure the spatial agglomerative characteristics of the FCR in 129 counties, this study used Stata 15 software to calculate the statistic values for seven periods and the annual average values (Table 6).

**Table 6.** Spatial correlation test results for FCR from 1990 to 2020.

Calculation Indicators	Year	1990	1995	2000	2005	2010	2015	2020	Annual Average
Moran's I	Values	0.60 ***	0.61 ***	0.61 ***	0.64 ***	0.65 ***	0.65 ***	0.65 ***	0.64 ***
	Z-Statistic	11.44	11.57	11.61	12.20	12.34	12.38	12.37	12.25
	p-Values	0.00	0.00	0.00	0.00	0.00	0.00	0.00	0.00
Geary's C	Values	0.38 ***	0.37 ***	0.38 ***	0.35 ***	0.36 ***	0.35 ***	0.35 ***	0.35 ***
	Z-Statistic	−10.33	−10.41	−10.40	−10.88	−10.81	−10.89	−10.93	−10.96
	p-Values	0.00	0.00	0.00	0.00	0.00	0.00	0.00	0.00
Getis and Ord's G	Values	0.05 ***	0.05 ***	0.05 ***	0.05 ***	0.04 ***	0.04 ***	0.04 ***	0.05 ***
	Z-Statistic	4.38	4.40	4.40	4.07	3.73	3.66	3.59	4.02
	p-Values	0.00	0.00	0.00	0.00	0.00	0.00	0.00	0.00

Note: \*\*\* indicates the significance levels of 1%.

As shown in Table 6, all the results pass the 1% significance level test, indicating that the FCRs of the 129 counties present obvious spatial agglomerative characteristics. Therefore, this study draws local Moran's I distribution maps of the annual average values of the FCRs in 129 counties (Figure 4).

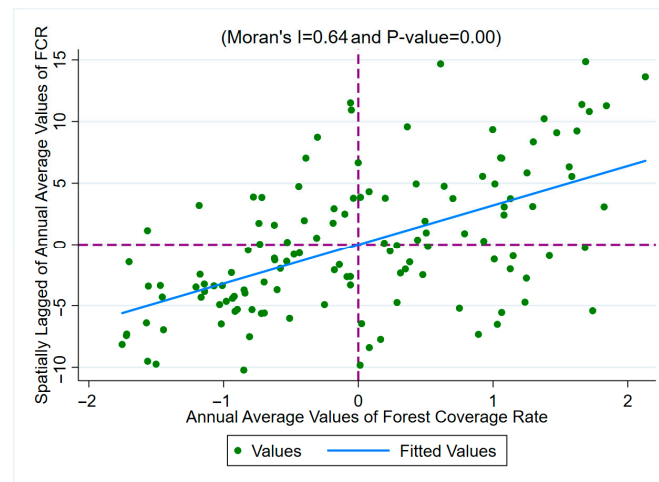


**Figure 4.** Distribution of annual average values of FCRs.

As can be seen in Figure 4, the estimated values for the 129 counties are mostly located in the first and third quadrants, and the slope of the basic linear fitting results is positive, indicating a significant positive spatial agglomeration of the FCR. In order to achieve a more detailed understanding of the agglomeration of these FCR, this study mapped the distribution of the annual average values of the FCRs and its cold & hot spots analysis results for 129 counties (Figure 5).

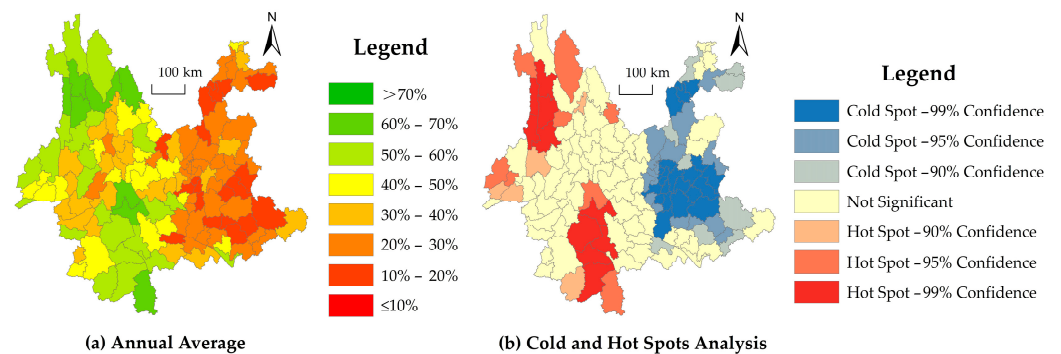


**Figure 5.** RS interpretation results and cold & hot spots analysis of annual average FCRs.

As shown in Figure 5, based on the annual average results, the distribution characteristics of the FCR still present a trend of lower in the east and higher in the west. The analysis of the cold & hot spots further confirmed the positive spatial agglomeration characteristics. Where, the main areas of prefectures, such as Kunming, Qujing, Yuxi, and Honghe, were located in the cold spot agglomeration area, which mainly presented the characteristics of having the agglomeration of low value and low value; the main regions of Xishuangbanna, Pu'er, Nujiang, Diqing, Dehong, and other prefectures were located in the hot spot agglomeration area, which mainly exhibited the features of having the agglomeration of high value and high value. It can be observed that the FCR in Yunnan has obvious spatial agglomerative characteristics, so it is particularly necessary to use spatially correlated research tools to analyze its influencing factors.

### 3.2. Analysis of Factors Influencing the FCR Based on Spatial Econometric Models

#### 3.2.1. Testing and Selection of Spatial Econometric Models

Prior to the construction of a spatial econometric model, it is essential to construct the OLS to test whether the model has significant spatial autocorrelation issues (Table 7).

**Table 7.** Spatial autocorrelation test results for the regression estimation.

Items	Calculation Indicators	Statistics	p-Values
Spatial Error	Moran’s I	2.68	0.01
	Lagrange Multiplier	132.21	0.00
	Robust Lagrange Multiplier	102.17	0.00
Spatial Lag	Lagrange Multiplier	33.57	0.00
	Robust Lagrange Multiplier	3.53	0.06

As shown in Table 7, although the LM statistic of the spatial lag term passes the 1% significance level test, the robust LM statistic does not pass the 5% significance level test, indicating that using the robust standard error method to estimate can alleviate the autocorrelation problem of the spatial lag term to some extent. However, all the test results of the spatial error term pass the 1% significance level test. It indicates that traditional OLS models suffer from severe spatial error autocorrelation issues. Therefore, compared to various different spatial econometric models, using the SEM to estimate will be able to better control the interference caused by spatial error autocorrelations, and it is the most suitable model.

### 3.2.2. Estimation Results and Analysis of Spatial Econometric Models

Although the aforementioned analysis method indicates that using the SEM is the most appropriate method, this study presents the results using the traditional panel and SAR models (Table 8). The reason for listing the results of other models is to further explore the robustness of the model. After inspection and testing, the regression results of this study have no model setting issues such as multicollinearity and heteroscedasticity. Considering that previous studies determined that the FCR in Yunnan was mainly characterized by lower in the east and higher in the west, this study divided the research area into the eastern and western regions of Yunnan and constructed the SEMs separately (the eastern region included Zhaotong, Kunming, Qujing, Wenshan, Yuxi, Chuxiong, and Honghe, and the other prefectures were included in the western region). In addition, this study calculated the average FCRs for 129 counties and divided their values into the lowest 50% and highest 50% according to their  $F_{CRs}$  to construct the appropriate models (Table 8). By comparing the SEM to other models, including classified models, it is not only conveniently to explore the robustness of the model, but also helped to better compare the differences in the effects of influencing factors in different FCR areas.

**Table 8.** Comparison of the estimation results of econometric models.

Variables	(1) Total Panel Model	(2) Total SAR	(3) Total SEM	(4) East SEM	(5) West SEM	(6) Lowest 50% SEM	(7) Highest 50% SEM
$\ln P_{GDP}$	3.2315 *** (0.2966)	1.4988 *** (0.2095)	2.8078 *** (0.2957)	2.6345 *** (0.3292)	3.3787 *** (0.3898)	2.3718 *** (0.3369)	3.9132 *** (0.3278)
$P_{OSI}$	0.0178 (0.0236)	0.0223 (0.0143)	−0.0031 (0.0168)	0.0314 (0.0202)	−0.0175 (0.0268)	0.0147 (0.0201)	0.0024 (0.0225)
$P_{OTI}$	−0.0172 (0.0107)	−0.0072 (0.0104)	−0.0151 (0.0168)	0.0106 (0.0196)	−0.0462 ** (0.0210)	−0.0081 (0.0200)	−0.0386 ** (0.0177)
$\ln P_D$	−3.4678 ** (1.3504)	−2.8705 *** (0.8173)	−5.2265 *** (0.9101)	−3.3115 *** (1.2599)	−1.7813 (1.4018)	−2.1366 * (1.1540)	−2.6498 ** (1.2715)
$P_{UR}$	0.0034 (0.0049)	−0.0027 (0.0050)	−0.0031 (0.0049)	−0.0021 (0.0048)	−0.0835 * (0.0441)	−0.0045 (0.0043)	−0.0144 (0.0372)



Table 8. Cont.

Variables	(1) Total Panel Model	(2) Total SAR	(3) Total SEM	(4) East SEM	(5) West SEM	(6) Lowest 50% SEM	(7) Highest 50% SEM
$R_{LR}$	−0.8374 *** (0.1085)	−0.6082 *** (0.1107)	−0.7839 *** (0.1229)	−0.6179 *** (0.1442)	−0.9049 *** (0.1898)	−0.4849 *** (0.1170)	−0.7725 *** (0.1944)
$P_{CLA}$	−0.7678 *** (0.2148)	−0.4834 *** (0.1031)	−0.4360 *** (0.1117)	−0.3554 *** (0.1184)	−0.8595* (0.5116)	−0.3807 *** (0.1062)	−0.3042 (0.2845)
$R_{LU}$	0.8351 *** (0.1392)	0.4484 *** (0.0731)	0.5806 *** (0.0779)	0.5010 *** (0.0873)	0.6883 *** (0.1441)	0.3552 *** (0.0820)	0.4870 *** (0.1381)
$P_{CCF}$	2.5004 *** (0.3101)	1.0263 *** (0.3319)	4.0295 *** (0.7415)	2.0522 *** (0.7530)	4.6380 *** (0.7339)	2.0055 ** (0.8165)	4.8906 *** (0.6049)
$R_{OR}$	0.0025 (0.0609)	−0.0315 (0.0325)	−0.0195 (0.0329)	0.0367 (0.0472)	−0.0351 (0.0473)	0.0029 (0.0414)	−0.0011 (0.0465)
$P_{BLA}$	0.1384 (0.2352)	0.3271 *** (0.1263)	0.0654 (0.1406)	0.2600 * (0.1484)	−0.3742 (0.3514)	0.0939 (0.1313)	−0.5436 (0.3783)
$P_{SE}$	−0.0080 (0.0386)	−0.0106 (0.0226)	−0.0695 ** (0.0272)	−0.0405 (0.0305)	−0.1914 *** (0.0564)	−0.0995 *** (0.0310)	−0.0466 (0.0389)
$P_{EI}$	0.0110 (0.0707)	−0.0018 (0.0559)	−0.0025 (0.0612)	−0.0985 (0.0812)	0.1564 * (0.0891)	−0.0795 (0.0667)	−0.0098 (0.0922)
$P_{MA}$	−0.0354 (0.1364)	−0.0434 (0.1119)	−0.0257 (0.1251)	−0.1137 (0.1434)	0.2603 (0.2561)	−0.1184 (0.1115)	−0.2028 (0.3038)
$P_{SSA}$	0.0059 (0.0588)	−0.0625 (0.0566)	−0.0160 (0.0639)	−0.0124 (0.0856)	0.0435 (0.0744)	−0.0378 (0.0692)	0.0224 (0.0694)
$A_{AT}$	0.5378 *** (0.1835)	0.3024 * (0.1628)	0.5947 *** (0.2297)	0.7587 ** (0.3178)	0.7340 ** (0.3006)	0.4456 (0.2916)	0.3111 (0.2678)
$A_{AP}$	−0.0016 ** (0.0008)	−0.0010 (0.0007)	−0.0007 (0.0014)	−0.0033 ** (0.0017)	−0.0004 (0.0014)	−0.0025 (0.0018)	0.0002 (0.0012)
$_{-cons}$	−35.2545 ** (16.4114)	−7.1738 (12.2214)	−3.5180 (14.046)	−5.1276 (17.1220)	−54.1026 * (29.6950)	8.0059 (15.0909)	7.3151 (31.7221)
Parameter $\rho$		0.5356 *** (0.0297)					
Parameter $\lambda$			0.6004 *** (0.0370)	0.4626 *** (0.0561)	0.3403 *** (0.0740)	0.5151 *** (0.0476)	0.2693 *** (0.0676)
Observations	903	903	903	518	385	448	455
R-squared	0.8543	0.6959	0.7182	0.5752	0.8049	0.4811	0.7348

Note: All estimation results are estimated by the robust standard error method. \*, \*\*, and \*\*\* indicate the significance levels of 10%, 5%, and 1%, respectively.

According to the test, the SEM is the optimal model. Therefore, this study will analyze the results estimated by the SEM and compare the estimation results of other models as well as the differences in the estimation results between regions with different FCRs. The results of  $\ln P_{GDP}$ ,  $\ln P_D$ ,  $R_{LR}$ ,  $P_{CLA}$ ,  $R_{LU}$ ,  $P_{CCF}$ ,  $P_{SE}$ , and  $A_{AT}$  are significant (Table 8), so this study will analyze these core influencing factors:

(1) The natural logarithmic form of the PCGDP ( $\ln P_{GDP}$ ). Based on the optimal SEM estimation results, the estimated coefficient is 2.8078 and passed the 1% significance level test, indicating that the PCGDP is a key factor affecting the FCR. Every 1% increase in the PCGDP will promote an increase of approximately 0.0281% in the  $F_{CR}$ . The results of both the panel and SAR models are significantly positive, indicating the robustness of the model. The significant positive correlation between  $\ln P_{GDP}$  and  $F_{CR}$  further indicates that economic growth is not the result of excessive deforestation and ecological damage. With the development of the economy, the awareness of the ecological protection has increased and it has more economic strength of afforestation to improve FCR and the ecology. The results of models 4–7 are significantly positive, but the absolute value of the estimated coefficient in the western region is higher than that in the eastern region, and the influence of  $\ln P_{GDP}$  on the  $F_{CR}$  is more significant in the highest 50% of FCR areas. It indicates that in areas with higher FCRs, fast economic development will be more conducive to improving

their FCRs, and the  $F_{CRs}$  in the west are generally higher than that in the east, so its effect will be more significant.

(2) The natural logarithmic form of population density ( $\ln P_D$ ). Based on the optimal SEM model estimation results, the coefficient is  $-5.2265$  and has passed the 1% significance level test, indicating that  $\ln P_D$  is a key factor affecting FCR. Every 1% increase in PD will lead to an about 0.0523% decrease in  $F_{CR}$ . The results of both panel model and SAR model are significantly negative, indicating the robustness of the model. The significant negative correlation between  $\ln P_D$  and  $F_{CR}$  is due to the fact that densely populated areas cause more deforestation, and with the process of urbanization, more and more forests will be converted into construction land to support the survival of people. The results of models 4–7 are all negative and most models are significant. Overall,  $\ln P_D$  has a more significant impact on  $F_{CR}$  in the eastern region and the highest 50% of FCR areas. This is mainly because many counties in the east have better economic conditions and a denser population, and the increase in population has a more significant impact on FCR. For areas with high FCRs, the impact of population growth will be more obvious.

(3) Land Reclamation Rate ( $R_{LR}$ ). Based on the optimal SEM model estimation results, the coefficient is  $-0.7839$  and has passed the 1% significance level test, indicating that  $R_{LR}$  is a key factor affecting FCR. Every 1% increase in  $R_{LR}$  will lead to a decrease of about 0.7839% in  $F_{CR}$ . The results of both panel model and SAR model are significantly negative with small difference, indicating the robustness of the model. The significant negative correlation between  $R_{LR}$  and  $F_{CR}$  is due to the increase in the proportion of cultivated land being transferred from other LUT, including the conversion of CFL to cultivated land. The results of models 4–7 are significantly negative, and overall,  $R_{LR}$  has a more significant impact on  $F_{CR}$  in the west and the highest 50% of FCR areas. This is mainly because the FCRs in these areas are generally high, and the phenomenon of converting closed forest land to cultivated land is more common.

(4) Proposal of Construction Land Area ( $P_{CLA}$ ). Based on the optimal SEM model estimation results, the coefficient is  $-0.4360$  and has passed the 1% significance level test, indicating that  $P_{CLA}$  is a key factor affecting FCR. Each 1% increase in  $P_{CLA}$  will lead to a decrease of about 0.4360% in  $F_{CR}$ . The results of both panel model and SAR model are significantly negative, indicating the robustness of the model. The significant negative correlation between  $P_{CLA}$  and  $F_{CR}$  is due to the fact that the increase in construction land often comes at the cost of occupying high-quality farmland or deforestation. With the rapid process of urbanization, more and more construction land is being used, occupying a considerable amount of closed forest land. The results of models 4–7 are all negative. Overall, the impact of  $P_{CLA}$  on  $F_{CR}$  is more significant (significance level of 1%) in the results of the east and the lowest 50% of FCR areas. This is mainly because the overall economic conditions in these areas are relatively good, and the expansion of construction land has occupied more closed forest land.

(5) Land Utilization Rate ( $R_{LU}$ ). Based on the optimal SEM model estimation results, the coefficient is 0.5806 and has passed the 1% significance level test, indicating that  $R_{LU}$  is a key factor affecting FCR. Every 1% increase in  $R_{LU}$  will promote an increase in  $F_{CR}$  by about 0.5806%. The results of both panel model and SAR model are significantly positive with small difference, indicating the robustness of the model. The significant positive correlation between  $R_{LU}$  and  $F_{CR}$  is due to the increase in land use efficiency, which helps to convert unused land into other LUT. As more and more land is effectively utilized, a significant amount of land will be converted into CFL, thereby increasing FCR and improving ecology. The results of models 4–7 are significantly positive, and overall,  $R_{LU}$  has a more significant impact on  $F_{CR}$  in the west and the highest 50% of FCR areas. This is mainly because the FCRs in these areas are generally high, and as more unused land is utilized reasonably, the proportion of land converted into closed forest land will be higher.

(6) The Conversion of Cropland to Forest Project ( $P_{CCF}$ ). Based on the optimal SEM model estimation results, the coefficient is 4.0295 and has passed the 1% significance level test, indicating that  $P_{CCF}$  is a key factor affecting FCR. With the experiment and

implementation of the CCFP policy in Yunnan in 2000,  $F_{CR}$  will increase by about 4.0295%. The results of both panel model and SAR model are significantly positive, indicating the robustness of the model. The results of models 4–7 are significantly positive, and overall,  $P_{CCF}$  has a more significant impact on  $F_{CR}$  in the west and the highest 50% of FCR areas. This is mainly because the overall terrain in these areas is relatively steep, with a higher proportion of  $\geq 25^\circ$  cultivated land. Therefore, the area of returning cultivated land to forests is larger, and the impact of this policy is more obvious.

(7) The Proposal of Soil Erosion Land Area ( $P_{SE}$ ). Based on the optimal SEM model estimation results, the coefficient is  $-0.0695$  and has passed the significance level test of 5%, indicating that  $P_{SE}$  is a key factor affecting FCR. Every 1% increase in  $P_{SE}$  will lead to a decrease of about 0.0695% in  $F_{CR}$ . The significant negative correlation between  $P_{SE}$  and  $F_{CR}$  is due to the fact that areas with a larger proportion of soil erosion often suffer more severe ecological damage, resulting in lower FCR. The results of models 4–7 are all negative and most models are significant. Overall, the impact of  $P_{SE}$  on  $F_{CR}$  is more significant in the west and the lowest 50% of FCR areas. This is mainly because the terrain in the west is relatively steep, especially in some areas with higher elevations in the northwest, which may suffer from greater ecological problems such as soil erosion; and soil erosion will bring greater harm for the areas with lower FCR.

(8) Annual Average Temperature ( $A_{AT}$ ). Based on the optimal SEM model estimation results, the coefficient is 0.5947 and has passed the 1% significance level test, indicating that  $A_{AT}$  is a key factor affecting FCR. Every 1% increase in  $A_{AT}$  will promote an increase in  $F_{CR}$  by about 0.5947%. The results of both panel model and SAR model are significantly positive, indicating the robustness of the model. The significant positive correlation between  $A_{AT}$  and  $F_{CR}$  is due to the fact that climate is an important factor affecting FCR, especially in areas with high temperatures and abundant precipitation, where trees are more likely to survive and the cost of afforestation will be lower. The results of models 4–7 are all negative and most models are significant. Overall, the difference in estimated coefficients among different regions is relatively small.

Although spatial econometric models can obtain accurate estimates of parameters based on controlling for spatial autocorrelation, simply dividing different FCR areas and constructing models separately cannot effectively determine the spatial differences and trends of key influencing factors. GWR can effectively compensate for this deficiency.

### 3.3. Results of the GWR Model

The GWR is a variable coefficient model. Compared with other spatial econometric models, its most prominent feature is to assign different estimation results to different regions, thereby better analyzing and answering the differences of the effects on the FCR and spatial change trends in terms of different regions. Based on it, this study takes the annual average values from the panel data of 7 periods (1990–2020) to construct a cross-sectional data for one period, and uses ArcGIS software and GWR4 software to construct the GWR model. After comparing the Adjust  $R^2$  values of multivariate GWR and univariate GWR, this paper uses multivariate GWR to determine the bandwidth according to the Akashi Information Criterion (AIC), and constructs a multivariate GWR model using stepwise regression method. Due to the fact that the  $P_{CCF}$  is a dummy variable, it needs to be excluded in the estimation of cross-sectional data. Given that reduce the dimensionality of panel data could lead to multicollinearity issues, this study excluded two independent variables (i.e. In  $P_D$  and  $A_{AT}$ ) from the core influencing factors mentioned above based on the principles of minimizing AIC value, maximizing Log Likelihood, and maximizing Adjust  $R^2$  value. The constructed GWR model has the Adjust  $R^2$  value of 0.77, the  $-2$  log likelihood value of 851.22, and the AIC value of 887.22, which is the best compared to other GWR models in the absence of multicollinearity problems and it is the optimal model. Based on it, this study applies GIS technology to output the regression results of its core factors (Figure 6), and conducts a detailed analysis based on the results.

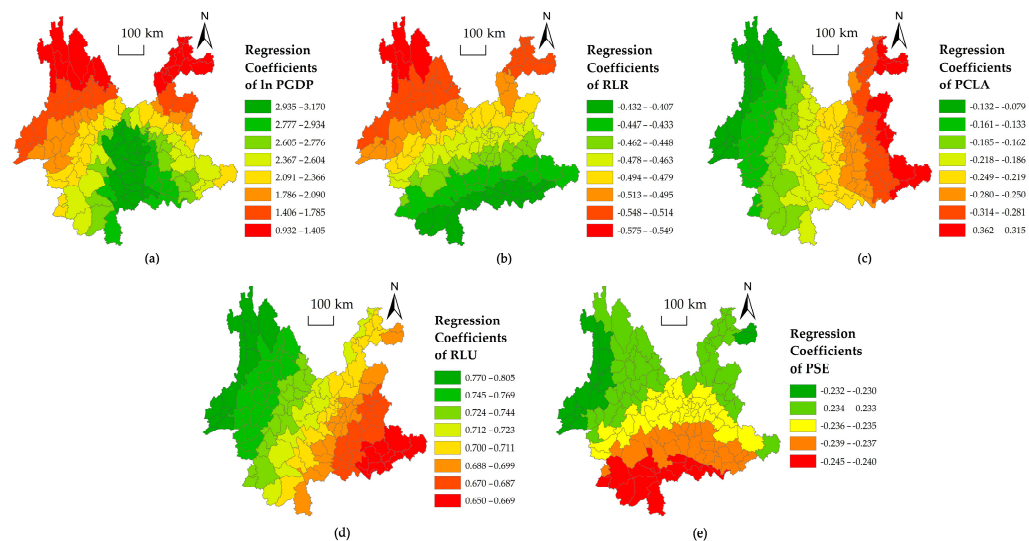


**Figure 6.** Results of the GWR model. (a) regression coefficients of  $\ln P_{GDP}$ ; (b) regression coefficients of  $R_{LR}$ ; (c) regression coefficients of  $P_{CLA}$ ; (d) regression coefficients of  $R_{LU}$ , and (e) regression coefficients of  $P_{SE}$ .

(1)  $\ln P_{GDP}$ . The estimated coefficients for each region are all positive, ranging from 0.932 to 3.170. The standard deviation of all estimated coefficients is 0.614, indicating a significant spatial heterogeneity in the effect of  $\ln P_{GDP}$  on  $F_{CR}$ . Overall, the effect shows a decreasing trend from the south to the northeast and northwest, which may be related to terrain and slope. Due to the terrain of Yunnan generally showing a trend of low in the south and high in the north, with the favorable conditions such as temperature in the south, these areas in the south will likely be planted with more trees with the development of the economy, so the impact of  $\ln P_{GDP}$  on  $F_{CR}$  in these areas will be more obvious.

(2)  $R_{LR}$ . The estimated coefficients for each region are negative, ranging from  $-0.407$  to  $-0.575$ . The standard deviation of all estimated coefficients is 0.037, indicating a certain degree of spatial heterogeneity in the effect of  $R_{LR}$  on  $F_{CR}$ . Overall, the effect shows a trend of increasing from the south to the north, which may also be related to terrain and slope. Due to the terrain of Yunnan generally showing a trend of low in the south and high in the north, there are more steep slope and high-altitude farmland in the north compared to the south, so the increase in the  $R_{LR}$  will have a more negative impact on  $F_{CR}$ .

(3)  $P_{CLA}$ . The estimated coefficients for each region are negative, ranging from  $-0.079$  to  $-0.362$ . The standard deviation of all estimated coefficients is 0.066, indicating a certain degree of spatial heterogeneity in the effect of  $P_{CLA}$  on  $F_{CR}$ . Overall, the effect shows a trend of increasing from the west to the east, which is similar to the previous results of spatial econometric regression. The reason may be that the economic conditions in the east are generally better than those in the west, and there is relatively more construction land, so the impact on  $F_{CR}$  will be more significant; the overall FCR in the west is relatively high, and the increase in construction land has a relatively small impact on it.

(4)  $R_{LU}$ . The estimated coefficients for each region are all positive, with a range of values between 0.650 and 0.805. The standard deviation of all estimated coefficients is 0.035, indicating a certain degree of spatial heterogeneity in the effect of  $R_{LU}$  on  $F_{CR}$ . Overall, the effect shows a decreasing trend from the northwest to the southeast, which is similar to the previous results. The reason may be that the karst rocky desertification problem in the southeast is more prominent, with a larger bare land area and relatively low land use efficiency. Therefore, the effect of  $R_{LU}$  on  $F_{CR}$  is relatively low; the FCR in the northwest is relatively high. With more land being used, the proportion of unused land converted into closed forest land may be larger.

(5)  $P_{SE}$ . The estimation coefficients for each region are all negative, with values ranging from  $-0.230$  to  $-0.245$ . The standard deviation of all estimation coefficients is

0.003, indicating that there is small spatial heterogeneity in the effect of  $P_{SE}$  on  $F_{CR}$ . Overall, the effect shows an increasing trend from the north to the southwest, which is similar to the previous results.

Although the GWR model can effectively reveal the regional differences in the effects of core influencing factors, in reality, different influencing factors are likely to be interrelated. Therefore, when multiple factors work together on  $F_{CR}$ , the total effect of these factors may not necessarily be equal to the sum of their single effects. In terms of exploring the joint effects of multiple influencing factors, the GD can appropriately answer the question of the correlation between different influencing factors.

### 3.4. Results of Geographic Detectors (GDs)

The GD can be applied to both single factor detection and double factor detection. For exploring the combined effects of multiple influencing factors on FCR, using GD for double factor detection is the most appropriate. Before using double factor detection, it is necessary to detect each single factor and the Q values of them (Table 9).

**Table 9.** Single-factor estimation results.

Factor	$\ln P_{GDP}$	$P_{OSI}$	$P_{OTI}$	$\ln P_D$	$P_{UR}$	$R_{LR}$	$P_{CLA}$	$R_{LU}$	$R_{OR}$	$P_{BLA}$	$P_{SE}$	$P_{EI}$	$P_{MA}$	$P_{SSA}$	$A_{AT}$	$A_{AP}$
Q Values	0.06	0.09	0.04	0.51	0.08	0.33	0.3	0.34	0.03	0.33	0.31	0.12	0.17	0.13	0.12	0.16

The results of it can only reflect the degree of independent influence of a single factor on FCR. To gain a more important results of the impact of multi factor interaction, this study used the double factor interaction detection of GD for analysis (Table 10). Meanwhile, referring to the classification types in Table 4, this study will reasonably classify the results of double factor detection (Table 11).

**Table 10.** Double-factor estimation results.

	$\ln P_{GDP}$	$P_{OSI}$	$P_{OTI}$	$\ln P_D$	$P_{UR}$	$R_{LR}$	$P_{CLA}$	$R_{LU}$	$R_{OR}$	$P_{BLA}$	$P_{SE}$	$P_{EI}$	$P_{MA}$	$P_{SSA}$	$A_{AT}$	$A_{AP}$
$\ln P_{GDP}$	0.22															
$P_{OSI}$	0.22	0.22														
$P_{OTI}$	0.57	0.59	0.58													
$\ln P_D$	0.17	0.28	0.18	0.56												
$P_{UR}$	0.43	0.44	0.44	0.59	0.41											
$R_{LR}$	0.45	0.42	0.42	0.54	0.41	0.45										
$P_{CLA}$	0.39	0.44	0.44	0.70	0.41	0.63	0.60									
$R_{LU}$	0.19	0.19	0.24	0.57	0.16	0.44	0.39	0.42								
$R_{OR}$	0.43	0.40	0.43	0.68	0.42	0.67	0.52	0.57	0.43							
$P_{BLA}$	0.51	0.49	0.47	0.67	0.44	0.58	0.57	0.52	0.39	0.61						
$P_{SE}$	0.26	0.27	0.21	0.56	0.27	0.41	0.40	0.48	0.24	0.47	0.48					
$P_{EI}$	0.34	0.30	0.26	0.55	0.28	0.42	0.35	0.54	0.28	0.44	0.56	0.27				
$P_{MA}$	0.33	0.24	0.24	0.61	0.23	0.45	0.38	0.56	0.28	0.48	0.54	0.30	0.22			
$P_{SSA}$	0.33	0.25	0.36	0.60	0.29	0.47	0.44	0.45	0.28	0.50	0.53	0.34	0.32	0.32		
$A_{AT}$	0.35	0.27	0.25	0.63	0.27	0.53	0.40	0.51	0.26	0.48	0.49	0.31	0.30	0.38	0.36	

From the results of double factor detection, there are only 2 types of detection results (i.e. NE and DE) (Table 11), indicating that the FCR is influenced by multiple factors, and the overlapping effects of these effects are more obvious. Where, it is very obvious that the interaction of  $\ln P_{GDP}$ ,  $P_{OSI}$ ,  $P_{OTI}$ ,  $P_{UR}$ ,  $P_{EI}$ , and  $R_{OR}$  with other factors has an impact on  $F_{CR}$  (mostly shows as the non-linear enhancement type), showing that the interaction effect of the 2 factors exceeds the sum of their single impact effects. The above results further indicate that the FCR is influenced by a combination of multiple factors, which exhibit complex, diverse, interwoven, and overlapping characteristics.

**Table 11.** Analysis and classification of the estimation results.

	$\ln P_{GDP}$	$P_{OSI}$	$P_{OTI}$	$\ln P_D$	$P_{UR}$	$R_{LR}$	$P_{CLA}$	$R_{LU}$	$R_{OR}$	$P_{BLA}$	$P_{SE}$	$P_{EI}$	$P_{MA}$	$P_{SSA}$	$A_{AT}$	$A_{AP}$
$\ln P_{GDP}$	NE															
$P_{OSI}$	NE	NE														
$P_{OTI}$	NE	NE	NE													
$\ln P_D$	DE	DE	NE													
$P_{UR}$	NE	NE	NE	DE												
$R_{LR}$	NE	NE	NE	DE	DE											
$P_{CLA}$	NE	NE	NE	DE	NE	DE										
$R_{LU}$	DE	NE	NE	DE	DE	DE	DE									
$R_{OR}$	NE	NE	NE	NE	NE	NE	NE	NE								
$P_{BLA}$	NE	DE	NE	DE	NE	NE	DE	DE	NE							
$P_{SE}$	NE	NE	NE	DE	NE	DE	DE	DE	NE	DE						
$P_{EI}$	NE	NE	NE	DE	NE	DE	DE	NE	NE	NE	NE					
$P_{MA}$	NE	NE	NE	DE	NE	DE	DE	NE	NE	DE	NE	DE				
$P_{SSA}$	NE	NE	NE	DE	NE	DE	DE	NE	NE	NE	NE	NE	DE			
$A_{AT}$	NE	NE	NE	DE	NE	DE	NE	DE	NE	NE	NE	NE	NE	NE		
$A_{AP}$	NE	NE	NE	DE	NE	NE	DE	NE	NE	DE	NE	NE	DE	NE	NE	

Note: "NE" and "DE" represent non-linear and double-factor enhancements, respectively.

Although the above analysis effectively reveals the interaction of various influencing factors, this study is more concerned with the specific changes of FCR in the future. Therefore, this study plans to use spatial econometric models to scientifically predict FCRs in 129 counties from 2025 to 2050.

### 3.5. Prediction Results for FCRs in 129 Counties in Yunnan Province from 2025 to 2050

The above analysis not only reveals the impact degree of factors on FCR, but also reveals the differences of the effects and the interaction effects. Therefore, based on the most suitable spatial econometric model mentioned above, referring to the research ideas and methods of Yang Renyi et al. (2021) [62] and Chen Qiang (2014) [49], this study uses OLS method to predict the results of various influencing factors from 2025 to 2050 ( $P_{CCF}$  takes 1 in 2000 and later), and fitting the panel data from 1990 to 2020 based on the most suitable SEM model, and predicting the FCRs of 129 counties from 2025 to 2050, and using GIS techniques to draw the predicted spatial distribution results (Figure 7).

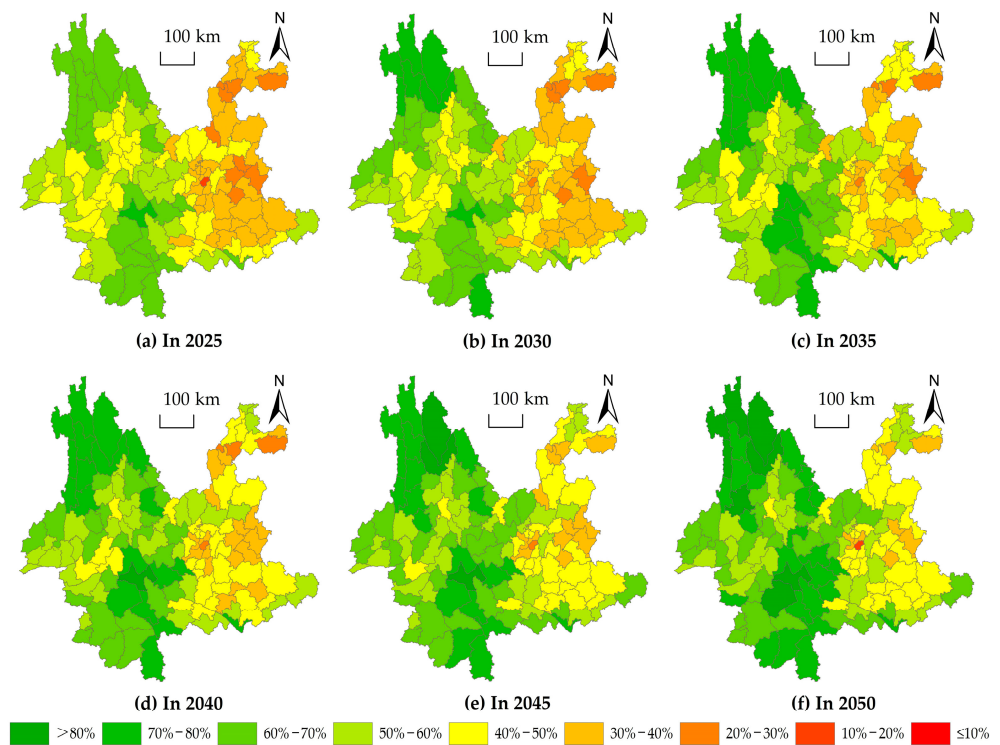


**Figure 7.** Prediction results of FCRs in 129 counties in Yunnan Province from 2025 to 2050.

From Figure 7, it can be seen that the distribution of the model prediction results of FCRs in 129 counties from 2025 to 2050 basically conforms to the spatiotemporal evolution law of 7 phases from 1990 to 2020. That is, in the future, the FCR will still show a trend of low in the east and high in the west, and the prediction results show that the FCR in each county is gradually improving. By 2050, the FCRs in the vast majority of western regions will reach over 50%. The above results further indicate that selecting the optimal spatial econometric model for prediction is more scientific and reasonable.

Although Figure 7 provides a more intuitive display of the predicted FCR distribution of 129 counties in the future, the map still cannot accurately show the data distribution and overall situation of the predicted FCR of each county. Therefore, the average, standard deviation, median and other indicators of the prediction results for each county in the next 6 phases are calculated (Table 12).

**Table 12.** Data description of prediction results of FCRs of 129 counties from 2025 to 2050.

Year	Mean	SD	P25	P50	P75	Min	Max
2025	47.03	12.80	36.68	46.12	56.81	19.63	72.42
2030	49.50	12.91	39.15	48.80	59.34	20.38	75.29
2035	51.96	13.03	41.51	51.33	61.88	21.06	78.17
2040	54.40	13.19	43.93	53.61	64.61	21.29	81.04
2045	56.78	13.41	46.44	55.79	67.56	20.02	83.92
2050	59.09	13.64	48.76	58.02	69.84	18.75	86.80
Average	53.13	13.76	42.81	52.40	63.84	18.75	86.80

Note: "Mean", "SD", "P25", "P50", "P75", "Min", and "Max" represent the average, standard deviation, lower quartile, median, upper quartile, minimum, and maximum of prediction values of forest coverage rate of 129 counties in Yunnan in the corresponding year, respectively.

From Table 12, it can also be seen that the FCRs of various counties are gradually increasing in 2025, which will mean that the fragile ecological environment in Yunnan will be improved. According to the prediction results, the average FCR of each county in Yunnan will reach 47.03% in 2025, and is expected to reach 59.09% by 2050. It is expected to net increase by 12.06% within 25 years (with an average annual increase of 0.48%). The results of statistical indicators such as median and maximum are also similar, showing a trend of increasing year by year. The only difference is the trend of the minimum  $F_{CR}$ , which the model shows will decrease to 18.75% in 2050. This is because with the acceleration of urbanization, more and more people from other prefectures will flow into some central city. This will not only exacerbate urban congestion, but also lead to a significant increase in construction land, which may cause a decrease in FCR.

#### 4. Discussion

Abundant FCR play an important central role in promoting ecological environment improvement and green development in a region. However, the existing research lacks the use of RS and GIS technology to systematically explore the spatiotemporal evolution of FCR in mountainous provinces in the long term, and also lacks the use of comprehensive measurement techniques and methods combined with RS image interpretation results and econometric model analysis to systematically discuss the influencing factors of FCR. In response to the shortcomings of the existing research, this study explored the spatiotemporal evolution characteristics and laws of FCR for 129 counties in Yunnan Province based on the LULC data obtained from seven periods RS image interpretation of Yunnan (i.e., 1990, 1995, 2000, 2005, 2010, 2015, and 2020), and combined diverse and systematic research methods, such as spatial econometric models, the GWR model, and the GD to reveal the influencing factors on FCR and predicted the FCRs from 2025 to 2050.

This study found that the FCRs in 129 counties significantly improved from 1990 to 2020, especially with large areas of other forest land, grassland, and unused land being transformed into closed forest land within 30 years, which significantly increased the FCR. This is commendable and also indicates that Yunnan has made significant progress in the

ECC in the past 30 years, and the fragile ecology has been significantly improved. However, this study still found that the FCRs in most areas in eastern Yunnan were significantly lower than those in western areas, and the reasons for this were varied. For some regions, such as Zhaotong in the northeast, a dense population was the main reason for the low FCR. The urbanization level and construction land in central Yunnan, including Kunming, Chuxiong, and Qujing, were relatively high. The economic development and urbanization process have had significant negative impacts on FCR. In the southeastern region of Yunnan, the inherently fragile ecological environment, such as karst rocky desertification, is an important factor restricting the FCR. In addition, the factors affecting FCR are complex and exhibit interactive and overlapping characteristics.

Although the research shows that the FCR in Yunnan has significantly improved in the past 30 years, it is still important to focus on the increase of FCR and improvement of ecological protection in the eastern region. We must not sacrifice a healthy ecological environment for high economic growth and rapid urbanization rates; we must not adopt the old perspective of pollution before treatment, allowing cities to excessively expand; and we also must not ignore forest and ecological issues in areas with better economic conditions. Yunnan Province has an important ecological location. The government should focus on the forest conditions in the eastern region, especially in ecologically fragile areas, and strive to increase FCR through afforestation and other methods, focusing on increasing the FCR and ecological environment conditions.

Some limitations were present in this study, which were mainly reflected in the following aspects: Firstly, due to the limitations in the data acquisition process, this study did not analyze the impacts of natural disasters, such as floods, landslides, and wildfires, as well as human activities, such as logging and agriculture, on FCR. Secondly, due to the limitations in obtaining RS image data, this study did not collect LULC data for each year to more accurately monitor the FCRs. Finally, the most recent data collected for this study was in 2020, this study did not further monitor the future changes of FCRs; thus, repeated comparisons and adjustments of the predicted results are needed in order to obtain more accurate prediction results. The aforementioned limitations must be continuously improved and expanded in the future research.

## 5. Conclusions

The study of FCR is related to the ecological environment and SDGs of a region. In response to the shortcomings of the existing research and the practical needs of the ECC in Yunnan Province, this study analyzed the spatiotemporal evolution and influencing factors of FCR for 129 counties in Yunnan Province from 1990 to 2020 based on the interpretation data of the seven-period RS data of LULCs and further predicted the FCR from 2025 to 2050:

(1) Although 0.3856 million hectares of closed forest land were converted into other land types over the last 30 years, there were still 8.1038 million hectares of other types of land converted into closed forest land, leading to the FCR in the whole Yunnan increasing from 28.96% in 1990 to 49.05% in 2020.

(2) In addition, the FCRs of 129 counties in Yunnan Province presented a clear spatial distribution pattern, showing an overall trend of lower in the east and higher in the west, with obvious spatial clustering characteristics.

(3) Furthermore, the analysis of influencing factors show that the increases of the per capita GDP ( $\ln P_{GDP}$ ), land utilization rate ( $R_{LU}$ ), and annual average temperature ( $A_{AT}$ ), and the implementation of the CCFP ( $P_{CCF}$ ) will significantly improve the  $F_{CR}$ , while the increases in the population density ( $\ln P_D$ ), land reclamation rate ( $R_{LR}$ ), and the proportion of construction land area ( $P_{CLA}$ ), and the proportion of soil erosion land area ( $P_{SE}$ ) will significantly reduce the  $F_{CR}$ .

(4) However, these core influencing factors present significant regional differences in terms of the results of the GWR model: the effect of  $\ln P_{GDP}$  on the FCR roughly shows a decreasing trend from the south to the northeast and northwest; the effect of the  $R_{LR}$  on the FCR roughly shows an increasing trend from the south to the north; the effect of



the  $P_{CLA}$  on the FCR roughly shows an increasing trend from the west to the east; the effect of the  $R_{LU}$  on the FCR roughly shows a decreasing trend from the northwest to the southeast; and the effect of the  $P_{SE}$  on the FCR roughly shows an increasing trend from the north to the southwest. Moreover, the FCR in Yunnan Province is influenced by a combination of multiple factors, which exhibit complex, diverse, interwoven, and overlapping characteristics, where the two-factor interaction between  $\ln P_{GDP}$ ,  $P_{OSI}$ ,  $P_{OTI}$ ,  $P_{UR}$ ,  $P_{EI}$ , and  $R_{OR}$  with other factors has a more significant impact on the FCR.

(5) Fortunately, the average FCR of each county in Yunnan Province will reach 47.03% in 2025 and is expected to reach 59.09% by 2050 according to the model prediction results. But the spatial pattern of FCR in Yunnan Province will still show a trend of appearing lower in the east and higher in the west in the future.

**Author Contributions:** Conceptualization, R.Y. and Z.Y.; methodology, R.Y., Y.H., C.Z. and Z.Y.; software, R.Y., Z.Y. and X.W.; validation, R.Y., Y.H., C.Z., Z.Y., M.X., X.W. and L.C.; formal analysis, R.Y. and Z.Y.; investigation, R.Y., Y.H., C.Z., Z.Y., M.X., X.W. and L.C.; resources, R.Y., Z.Y. and X.W.; data curation, R.Y., Y.H., C.Z., Z.Y. and X.W.; writing—original draft preparation, R.Y., Y.H., C.Z., Z.Y., M.X., X.W. and L.C.; writing—review and editing, R.Y., Y.H., C.Z., Z.Y., M.X., X.W. and L.C.; visualization, Z.Y. and C.Z.; supervision, Z.Y. and C.Z.; project administration, Z.Y. and C.Z.; funding acquisition, Z.Y. and C.Z. All authors have read and agreed to the published version of the manuscript.

**Funding:** This study was funded by the National Natural Science Foundation of China (41261018), the National Natural Science Foundation of China (71673182), and the Major Projects of National Social Science Foundation of China (18VJ023).

**Data Availability Statement:** The RS image data in this research were collected from “<https://www.resdc.cn/>” (accessed on 18 January 2023). The DEM data were collected from “[http://www.gscloud.cn](http://www.gscloud.cn/)” (accessed on 25 February 2023). The county boundaries of Yunnan Province were collected from “<https://yunnan.tianditu.gov.cn/MapResource>” (accessed on 7 March 2023). The economic and social statistical data were collected from “<https://stats.yn.gov.cn/List22.aspx>” (accessed on 17 May 2023), “<http://www.stats.gov.cn/sj/ndsj/>” (accessed on 3 June 2023), and the EPS platform (website: “<https://www.epsnet.com.cn/index.html#/Index>”) (accessed on 9 October 2023).

**Conflicts of Interest:** The authors declare no conflicts of interest.

## References

- Chen, D.L.; Jin, M.M. Study on Temporal and Spatial Distribution Law of the Forest Coverage of China and Its Influence on Air Quality. *J. Hebei For. Sci. Technol.* **2016**, *44*, 52–55+68.
- Zheng, Y.; Li, S.; Kanran, T.; Ma, X.J.; Qian, R. Effect of Forest Coverage Rate and Other Influencing Factors on PM 2.5—Taking Panel Data Model of 13 Cities (Districts) in Heilongjiang Province as Example. *J. Northeast. For. Univ.* **2020**, *48*, 64–70.
- Bonan, G.B. Forests and climate change: Forcings, feedbacks, and the climate benefits of forests. *Science* **2008**, *320*, 1444–1449. [[CrossRef](#)] [[PubMed](#)]
- Xiao, Y.F. The spatiotemporal distribution pattern of forest coverage in China and its impact on air quality. *Contemp. Hortic.* **2020**, *27*, 162–163.
- Yang, R.Y.; Zhong, C.B. Analysis on Spatio-Temporal Evolution and Influencing Factors of Air Quality Index (AQI) in China. *Toxics* **2022**, *10*, 712. [[CrossRef](#)] [[PubMed](#)]
- Ran, X.O. Analysis and Reflection on Improving Forest Coverage. *J. Green Sci. Technol.* **2016**, *18*, 83–84.
- Yang, Z.S. *Study on Land Use Changes and Its Ecological Effects in Different Landform Areas of Yunnan Province Driven by China's Project of Converting Farmland to Forest*, 1st ed.; China Science and Technology Press: Beijing, China, 2011.
- Guan, Y.X. Analysis of Factors Influencing Forest Coverage in Fujian Province and Research on Countermeasures. *For. Prospect. Des.* **2015**, *35*, 10–13.
- Zhang, J.T.; Mai, Q.S. Evaluation of Economic Value of Forest Carbon Sequestration in Yunnan Province. *J. Green Sci. Technol.* **2022**, *24*, 264–268.
- Hansen, M.C.; Roy, D.P.; Lindquist, E.; Adusei, B.; Justice, C.O.; Altstatt, A. A method for integrating MODIS and Landsat data for systematic monitoring of forest cover and change in the Congo Basin. *Remote Sens. Environ.* **2008**, *112*, 2495–2513. [[CrossRef](#)]
- Kennedy, R.E.; Yang, Z.; Cohen, W.B.; Pfaff, E.; Braaten, J.; Nelson, P. Spatial and temporal patterns of forest disturbance and regrowth within the area of the Northwest Forest Plan. *Remote Sens. Environ.* **2012**, *122*, 117–133. [[CrossRef](#)]
- Cohen, W.B.; Yang, Z.; Kennedy, R. Detecting trends in forest disturbance and recovery using yearly Landsat time series: 2. TimeSync—Tools for calibration and validation. *Remote Sens. Environ.* **2010**, *114*, 2911–2924. [[CrossRef](#)]

13. Wang, K. *Analysis of the Changes of Forest Resources and the Related Driving Force in Shandong Province*, 1st ed.; Shandong Agricultural University: Tai'an, China, 2016.
14. Ma, J.J.; Gao, M.L.; Li, Z.H.; Xu, H.H.; Peng, J.B. Spatial and temporal changes of forest cover and its driving factors over the Yellow River basin. *Bull. Surv. Mapp.* **2023**, *69*, 51–57.
15. Verbesselt, J.; Robinson, A.; Stone, C.; Culvenor, D. Forecasting tree mortality using change metrics derived from MODIS satellite data. *For. Ecol. Manag.* **2009**, *258*, 1166–1173. [[CrossRef](#)]
16. Pflugmacher, D.; Cohen, W.B.; Kennedy, E.R. Using Landsat-derived disturbance history (1972–2010) to predict current forest structure. *Remote Sens. Environ.* **2012**, *122*, 146–165. [[CrossRef](#)]
17. Li, Y.; Xue, C.Y.; Shao, H.; Shi, G.; Jiang, N. Study of the Spatiotemporal Variation Characteristics of Forest Landscape Patterns in Shanghai from 2004 to 2014 Based on Multisource Remote Sensing Data. *Sustainability* **2018**, *10*, 4397. [[CrossRef](#)]
18. Zhang, Y.J.; Wang, L.; Zhou, Q.; Tang, F.; Zhang, B.; Huang, N.; Nath, B. Continuous Change Detection and Classification—Spectral Trajectory Breakpoint Recognition for Forest Monitoring. *Land* **2022**, *11*, 504. [[CrossRef](#)]
19. Yin, H.Y.; Zhang, Z.W.; Yang, X.L.; Du, T.; Tang, Y.F.; Zhou, Y.Z. Statistical Analysis of Forest Coverage Based on ETM Images: A Case Study of Bayi District in Linzhi City. *Jiangsu Agric. Sci.* **2020**, *48*, 260–265.
20. Kennedy, R.E.; Yang, Z.; Cohen, W.B. Detecting trends in forest disturbance and recovery using yearly Landsat time series: 1. LandTrendr-Temporal segmentation algorithms. *Remote Sens. Environ.* **2010**, *114*, 2897–2910. [[CrossRef](#)]
21. Gao, Y.; Yuan, J.H.; Gong, X.W.; Li, Y.P.; Xiao, W.; Ren, G.P. A Cost-Effective Approach to Estimating Forest Coverage over Mountainous Regions Based on Google Earth: A Case Study in Yunnan. *J. Dali Univ.* **2019**, *4*, 62–68.
22. Shi, R.Y.; Wang, H.F. Study on change of forest coverage based on TM image. *Mine Surv.* **2019**, *47*, 69–72+112.
23. Zhang, W.B.; Gao, F.; Jiang, N.; Zhang, C.; Zhang, Y.C. High-Temporal-Resolution Forest Growth Monitoring Based on Segmented 3D Canopy Surface from UAV Aerial Photogrammetry. *Drones* **2022**, *6*, 158. [[CrossRef](#)]
24. Li, Q.L. *Spatial-Temporal Characteristics and Driving Forces of Forestland Changes in the Yangtze River Economic Belt*, 1st ed.; Southwest University: Chongqing, China, 2023.
25. Zhao, X.D.; Li, L.C.; Yang, W.T.; Cheng, B.D.; Liu, J.L. Analysis of Socio-Economic Influencing Factors of Forest Transition in Counties of Fujian Province. *Sci. Silvae Sin.* **2019**, *55*, 147–156.
26. Wu, W.G.; Zhu, Y.; Wang, Y.F. Spatio-Temporal Pattern, Evolution and Influencing Factors of Forest Carbon Sinks in Zhejiang Province, China. *Forests* **2023**, *14*, 445. [[CrossRef](#)]
27. Kirton, J.; Kokotsis, E.; Warren, B. Reconfiguring the Global Governance of Climate Change. *Taylor Fr.* **2021**, *47*, 121–123.
28. Brown, S.; Lugo, A.E. Biomass of tropical forests: A new estimate based on forest volumes. *Science* **1984**, *223*, 1290–1293. [[CrossRef](#)]
29. Zhang, X.D. Ways to increase forest coverage. *Friends Farmers Becom. Rich* **2016**, *23*, 322.
30. Deng, H.P.; Wang, Q.; Dan, L. Impacts of Climate on Forest—Runoff Relationship. *J. Water Resour. Water Eng.* **2018**, *29*, 18–24.
31. Wang, K.; Chen, T.; Luo, J.W.; Biao, J.L.; Wang, D.; Lu, F.D. Analysis on the Relationship between the Change of Forest Resources and Per Capita GDP in Shandong Province Based EKC Model. *Issues For. Econ.* **2016**, *36*, 222–226.
32. Zhang, Q. *Research on Forest Resources Abundance and Economic Development in the Yangtze River Delta*, 1st ed.; Nanjing Forestry University: Nanjing, China, 2016.
33. Jiang, Y.Y.; Du, W.T.; Chen, J.Z.; Wang, C.Y.; Wang, J.N.; Sun, W.X.; Chai, X.; Ma, L.J.; Xu, Z.L. Climatic and Topographical Effects on the Spatiotemporal Variations of Vegetation in Hexi Corridor, Northwestern China. *Diversity* **2022**, *14*, 370. [[CrossRef](#)]
34. Hu, W.P.; Long, T.W. Analysis on the Causes of Yunnan Province Forest Cover Decline in 2021. *For. Investig. Des.* **2023**, *52*, 12–15.
35. Mizuno, T.; Kojima, N.; Asano, S. The risk reduction effect of sediment production rate by understory coverage rate in granite area mountain forest. *Sci. Rep.* **2021**, *11*, 14415. [[CrossRef](#)]
36. Hefeeda, M.; Bagheri, M. Forest Fire Modeling and Early Detection using Wireless Sensor Networks. *Ad Hoc Sens. Wirel. Netw.* **2009**, *7*, 169–224.
37. Yuan, X. Dynamic grey forecast of forest resources in Jiangxi Province. *Hubei Agric. Sci.* **2022**, *61*, 152–156.
38. Gu, K.P. Structure and Simulating of the National Forest Resources Prediction Model. *J. Beijing For. Univ.* **1988**, *10*, 57–66.
39. Office of Yunnan Provincial Agricultural Zoning Commission. *Land Area of Different Climatic Zones and Slopes in Yunnan Province*, 1st ed.; Yunnan Science and Technology Press: Kunming, China, 1987.
40. National Bureau of Statistics. *China Statistical Yearbook 2021*, 1st ed.; China Statistics Press: Beijing, China, 2021.
41. Xu, X.L.; Liu, J.Y.; Zhang, S.W.; Li, R.D.; Yan, C.Z.; Wu, S.X. Multi-period land use and land cover monitoring data set in China (CNLUCC). In *Resource and Environment Science Registration and Publication System*; Institute of Geographic Sciences and Natural Resources Research, Chinese Academy of Sciences: Beijing, China, 2018. Available online: <http://www.resdc.cn/DOI> (accessed on 8 February 2022).
42. Liu, J.Y.; Liu, M.L.; Deng, X.Z.; Zhuang, D.F.; Zhang, Z.X.; Luo, D. The land use and land cover change database and its relative studies in China. *J. Geograph. Sci.* **2002**, *12*, 275–282.
43. Liu, J.Y.; Liu, M.L.; Zhuang, D.F.; Zhang, Z.X.; Deng, X.Z. Study on spatial pattern of land-use change in China during 1995–2000. *Sci. China (Ser. D)* **2003**, *46*, 373–384. [[CrossRef](#)]
44. Liu, J.Y.; Kuang, W.H.; Zhuang, Z.X.; Xu, X.L.; Qin, Y.W.; Ning, J.; Zhou, W.C.; Zhang, S.W.; Li, R.D.; Yan, C.Z.; et al. Spatio-temporal characteristics, patterns and causes of land-use changes in China since the late 1980s. *J. Geograph. Sci.* **2014**, *24*, 195–210. [[CrossRef](#)]

45. Kuang, W.H.; Zhang, S.W.; Du, G.M.; Yan, C.Z.; Wu, S.X.; Li, R.D.; Lu, D.S.; Pan, T.; Ning, J.; Guo, C.Q.; et al. Remotely sensed mapping and analysis of spatio-temporal patterns of land use change across China in 2015–2020. *Acta Geograph. Sin.* **2022**, *77*, 1056–1071.
46. Yang, Z.S.; Yang, S.Q.; Yang, R.Y.; Wu, Q.J. A Study on Spatiotemporal Changes of Ecological Vulnerability in Yunnan Province Based on Interpretation of Remote Sensing Images. *Diversity* **2023**, *15*, 963. [[CrossRef](#)]
47. He, B.W.; Li, D.; Liu, X.J. Regional differentiation characteristics and the influencing factors of spatial poverty in rural areas of Gansu Province. *Res. Agric. Mod.* **2019**, *40*, 819–829.
48. Yang, Z.S.; Yang, R.Y.; Liu, F.L. Spatio-temporal evolution and influencing factors of urban-rural income gap in Yunnan Province based on poverty classification. *Geogr. Res.* **2021**, *40*, 2252–2271.
49. Chen, Q. *Advanced Econometrics and Stata Application*, 2nd ed.; Higher Education Press: Beijing, China, 2014.
50. Moran, P. Notes on Continuous Stochastic Phenomena. *Biometrika* **1950**, *37*, 17–23. [[CrossRef](#)]
51. Geary, R. The Contiguity Ratio and Statistical Mapping. *Inc. Stat.* **1954**, *5*, 115–145. [[CrossRef](#)]
52. Getis, A.; Ord, J. The Analysis of Spatial Association by Use of Distance Statistics. *Geogr. Anal.* **1992**, *24*, 189–206. [[CrossRef](#)]
53. Yang, R.Y.; Zhong, C.B.; Yang, Z.S.; Liu, F.L.; Peng, H.Y. Analysis on Poverty Influencing Factors in Deep Poverty County of Karst Rocky-desertified Area in Southwest China. *World Reg. Stud.* **2022**, *31*, 1298–1309.
54. Fotheringham, A.S.; Brunson, C. Local forms of spatial analysis. *Geogr. Anal.* **1999**, *31*, 340–358. [[CrossRef](#)]
55. Yang, W.Y.; Li, T.; Cao, X.S. The spatial pattern of Community Travel Low Carbon Index (CTLCI) and spatial heterogeneity of the relationship between CTLCI and influencing factors in Guangzhou. *Geogr. Res.* **2015**, *34*, 1471–1480.
56. Shui, W.; Du, Y.; Chen, Y.P.; Jian, X.M.; Fan, B.X. Spatial patterns and influence factors of specialization in tea cultivation based on geographically weighted regression model: A case study of Anxi county of Fujian province, China. *J. Appl. Ecol.* **2017**, *28*, 1298–1308.
57. Wu, P.; Li, T.S.; Li, W.M. Spatial differentiation and influencing factors analysis of rural poverty at county scale: A case study of Shanyang county in Shaanxi province, China. *Geogr. Res.* **2018**, *37*, 593–606.
58. Wang, J.F.; Li, X.H.; Christakos, G.; Liao, Y.L.; Zhang, T.; Gu, X.; Zheng, X.Y. Geographical detectors-based health risk assessment and its application in the neural tube defects study of the Heshun region, China. *Int. J. Geogr. Inf. Sci.* **2010**, *24*, 107–127. [[CrossRef](#)]
59. Wang, J.F.; Xu, C.D. Geodetector: Principle and prospective. *Acta Geogr. Sin.* **2017**, *72*, 116–134.
60. Liao, Y.; Wang, X.Y.; Zhou, J.M. Suitability assessment and validation of giant panda habitat based on geographical detector. *J. Geoinf. Sci.* **2016**, *18*, 767–778.
61. Huang, Q.; Li, J.P.; Zheng, Z.; Xu, J. The application of natural breakpoint method in the classification and grading management evaluation system of materials and equipment. *Hous. Real Estate* **2023**, *9*, 44–48.
62. Yang, R.Y.; Liu, F.L.; Yang, Z.S. Prediction and Protection of Cultivated Land in China. *Asian Agric. Res.* **2021**, *13*, 3–7.

**Disclaimer/Publisher’s Note:** The statements, opinions and data contained in all publications are solely those of the individual author(s) and contributor(s) and not of MDPI and/or the editor(s). MDPI and/or the editor(s) disclaim responsibility for any injury to people or property resulting from any ideas, methods, instructions or products referred to in the content.